Density-functional perturbation theory with ultrasoft pseudopotentials

Andrea Dal Corso
Scuola Internazionale Superiore di Studi Avanzati (SISSA) via Beirut 2/4, I-34014 Trieste, Italy and INFM, Unità di Trieste, Trieste, Italy
(Received 18 June 2001; published 28 November 2001)

Density-functional perturbation theory for lattice dynamics is presented in a general framework which includes Vanderbilt's ultrasoft pseudopotentials, nonlinear exchange and correlation core corrections, the local spin-density approximation, and spin-polarized generalized gradient corrections. The dynamical matrices of metallic and of insulating solids are calculated at arbitrary wave vectors. The method is applied to the Cu(001) surface and to the nitrobenzene molecule.

DOI: 10.1103/PhysRevB.64.235118 PACS number(s): 71.15.Mb, 63.20.Dj

I. INTRODUCTION

In the last ten years, *ab initio* calculations of the phonon-dispersion spectra of solids and surfaces have complemented the empirical Born–von Karman force-constant models in interpreting and explaining the experimental data, thanks to the introduction of density-functional perturbation theory (DFPT).[1,2] This technique, based on density-functional theory (DFT), allows the efficient treatment of the response of an electron system to external perturbations. The phonon frequencies are obtained at arbitrary wave vectors of the Brillouin zone (BZ) with an effort which is almost wavelength independent and comparable, for each mode, to the effort required to calculate the ground state of the unperturbed system. At present, there are several implementations of DFPT for lattice dynamics which apply different formulas for the interatomic force constants and reflect the peculiarities of the scheme employed for the solution of the DFT equations.

In the Born-Oppenheimer approximation, the interatomic force constants are identified with the second-order energy derivatives with respect to atomic displacements. In DFT, the energy is a functional of the electronic charge density and a minimum variational principle gives the ground-state density. As a consequence, also the even-order energy derivatives are variational.[3] In practice, the energy minimization is carried out on the Kohn and Sham (KS) functional which depends on single-particle orbitals subject to orthonormalization constraints. The Taylor expansion of the energy functional and the Lagrange multipliers technique lead to variational expressions for the second-order energy derivatives which can be regarded as functionals of the first-order wave-function derivatives. The minimization of the second-order energy[3] shows that the first-order wave-function derivatives are the solution of a self-consistent Sternheimer linear system. The same conclusion is reached also via standard perturbation theory applied to the KS equations.[1] In some implementations, the solution of the self-consistent linear system is entirely avoided via a direct minimization of the second-order energy.[4,5]

The interatomic force constants can be calculated also by differentiation of the Hellmann-Feynman (HF) forces.[6] This procedure leads to expressions which are not variational. Nevertheless, in this way, the mixed second-order energy derivatives depend on the first-order wave-function derivatives due to a single perturbation. Thus the response to one phonon allows the evaluation of a full row of the dynamical matrix. This approach, introduced in the first implementation of DFPT,[1,7] has been generalized to metallic systems as well.[8]

DFPT turns out to be simple to implement with a plane-waves (PW's) basis set and norm conserving (NC) pseudopotentials (PP's).[9,10] The only drawback is that PW's are not efficient enough to describe first-row elements or transition metals and for these applications all-electron methods,[11–13] or mixed basis[14] have been extensively applied in the past. DFPT has been presented in the framework of the linearized augmented PW method (LAPW),[15] of the linear muffin tin orbitals (LMTO) scheme,[16] and with mixed basis.[17] Several applications of these methods have been reviewed in Ref. 2.

More recently, Vanderbilt's ultrasoft (US) PP's (Ref. 18) have been demonstrated capable to deal with localized electrons and to provide results which are often as accurate as those obtained with the all-electron methods. This paper is devoted to the presentation of DFPT in the framework of US PP's. Its purpose is to provide all the details needed to implement the method with a PW basis set. In Ref. 19, DFPT with US PP's has been briefly described, the discussion was focused on insulating systems whereas the treatment of metals was only sketched. In this paper, I start from an energy functional which applies to metallic systems, as well as to insulators. Spin polarization is included in the energy functional for the study of magnetic materials and the exchange and correlation energy functional depends on the total spin charge densities n_σ and on their gradients ∇n_σ. The total spin charge densities are obtained by adding a pseudized core charge to the valence charge densities as in the nonlinear core correction (NLCC) approximation.[20] This scheme comprises several different recipes for the generalized gradient approximation (GGA), and the local spin-density approximation (LSDA) is recovered by neglecting ∇n_σ in the exchange and correlation energy. The orbitals are subject to generalized orthonormalization constraints with an overlap matrix which varies in response to small atomic displacements. Furthermore the charge density is calculated with an augmentation term as in the US PP scheme. The interatomic force constants are obtained by differentiation of the HF forces and the induced spin charge densities and the first-

order wave-function derivatives are discussed in detail.

The formulas obtained in this paper have been applied to the calculation of the phonon dispersions of Cu, Ag, and Au in Ref. 19, and of Si, C, Cu, and Al in Ref. 21. In the latter reference, the performances of the local-density approximation (LDA) and of the GGA have been compared. The phonons of magnetic bcc iron and fcc nickel have been presented in Ref. 22 and the vibrational properties of the Cu(001)/CO system have been discussed in Ref. 23. In this paper the theory is illustrated with two examples: the Cu(001) surface and the nitrobenzene molecule. First, I analyze the interatomic force constants at the Cu(001) surface and within the bulk, comparing the results of the LDA and the ones of the GGA. Second, the vibrational modes of a finite Cu(001) slab are calculated, the surface modes of the slab are identified and discussed together with the available experimental data. The nitrobenzene molecule is simulated in a cubic supercell, all its vibrational modes are calculated and the theoretical frequencies are compared with data provided by infrared and Raman spectroscopies.

This paper is organized as follows. In Sec. II, the DFT energy, the KS equations, and the HF forces are written for the US PP's scheme. Section III deals with the charge density linearly induced by a perturbation, Sec. IV with the generalized Sternheimer equation, and Sec. V with the mixed second-order energy derivatives. The vibrational properties of the Cu(001) surface are presented in Sec. VI and the vibrational spectra of the nitrobenzene molecule is discussed in Sec. VII. In the paper, the notation is kept as simple as possible in order to focus on the new features of the US PP's scheme. The notation is simplified by considering a general quantum system, a general perturbation and general nonlocal PP's. The appendixes report detailed expressions implementable in an electronic structure code. In Appendix A, the formulas for the second-order energy derivatives, specialized to a periodic solid, a phonon perturbation and US PP's, are used to calculate the dynamical matrices at an arbitrary **q** point of the BZ. At this level the basis functions used to expand the orbitals are not relevant, provided that they do not depend on the ionic positions, as the PW's, so that Pulay-type corrections[24] are not needed. Finally in Appendix B, I introduce the PW basis set. The formula of this Appendix have been implemented in a code based on PW's and US PP's.[25]

II. GROUND-STATE ENERGY AND IONIC FORCES

According to the Hohenberg and Kohn theorem,[26] the energy of a system of N_{el} interacting electrons in the potential of the ions is a unique functional of the electronic charge density and it is minimized by the ground-state density. An explicit form for this functional has been given by Kohn and Sham who introduced an auxiliary system of N_{el} noninteracting electrons with the same density of the interacting system. The charge density of the noninteracting electrons has a unique representation in terms of single-particle electronic orbitals $\{\psi_{i\sigma}(\mathbf{r})\}$ (the index i labels the electronic energy levels, and σ the spin state), and the energy of the interacting system becomes a functional of these orbitals. The generalization of this scheme to energy functionals with fractional occupations and spin polarization[27] allows the description of open as well as closed-shell finite systems or metallic as well as insulating crystalline solids. I choose a functional which includes a term that makes it variational even with variable occupations.[28,29,8] A smearing approach is used and the occupation numbers are functions of the energy levels $\varepsilon_{i\sigma}$ and of the Fermi energy ε_F which fixes the electron number. The ionic positions act as external parameters for the functional. In the US PP's scheme, the energy has four contributions:

$$F_{tot}=E[\{\psi_{i\sigma}(\mathbf{r})\}]+F[\rho_\sigma(\mathbf{r}),\rho_{c,\sigma}(\mathbf{r})]+U_{II}+\sum_{i\sigma}\eta\tilde{\theta}_1\left(\frac{\varepsilon_F-\varepsilon_{i\sigma}}{\eta}\right). \quad (1)$$

In order to establish a uniform notation, these four terms are recalled in this section. All equations are in atomic units: the Planck constant $\hbar=1$, the electron charge $e^2=1$, and the electron mass $m_e=1$. The energy is measured in Hartree.

The first term in Eq. (1) is

$$E[\{\psi_{i\sigma}(\mathbf{r})\}]=\sum_{i\sigma}\tilde{\theta}\left(\frac{\varepsilon_F-\varepsilon_{i\sigma}}{\eta}\right)\langle\psi_{i\sigma}|-\frac{1}{2}\nabla^2+V_{NL}|\psi_{i\sigma}\rangle, \quad (2)$$

where the index i runs over all electronic states. $\tilde{\theta}$ is an approximation of the Fermi function, thus in practice, this sum extends to the completely filled orbitals in insulators and also to some partially filled states above the Fermi energy in metals. The form of $\tilde{\theta}$ depends on the smearing technique and on a smearing parameter η. For vanishing η, it coincides with the step function. Examples of $\tilde{\theta}$ functions are found in Refs. 30 and 31, where the smearing approximation is introduced by defining the shape of the Dirac delta function $\tilde{\delta}(x)$ while $\tilde{\theta}(x)=\int_{-\infty}^{x}\tilde{\delta}(y)dy$. V_{NL} is the nonlocal part of the PP which, in the US PP's scheme, reads

$$V_{NL}(\mathbf{r}_1,\mathbf{r}_2)=\sum_{Inm}D_{nm}^{(0)\gamma(I)}\beta_n^{\gamma(I)}(\mathbf{r}_1-\mathbf{R}_I)\beta_m^{*\gamma(I)}(\mathbf{r}_2-\mathbf{R}_I), \quad (3)$$

where the projector functions $\beta_m^{\gamma(I)}(\mathbf{r})$ and the coefficients $D_{nm}^{(0)\gamma(I)}$ characterize the PP for each atomic type $\gamma(I)$. They are obtained by atomic calculations as discussed in Ref. 18. The index I labels the ionic positions $\mathbf{R}_I$. The indexes n and m run over the β functions. In the Kleinman Bylander (KB) (Ref. 10) separable NC PP's scheme, the nonlocal part of the PP is written as in Eq. (3), but with only diagonal $D_{nn}^{(0)\gamma(I)}$ coefficients. In both cases, the meaning of the bra-ket notation in Eq. (2) is: $\langle\psi_{i\sigma}|V_{NL}|\psi_{i\sigma}\rangle=\int d^3r_1d^3r_2\psi_{i\sigma}^*(\mathbf{r}_1)V_{NL}(\mathbf{r}_1,\mathbf{r}_2)\psi_{i\sigma}(\mathbf{r}_2)$.

The second term in Eq. (1), F, is a functional of the spin-up and spin-down valence electron charge densities:

$$\rho_\sigma(\mathbf{r})=\sum_i\tilde{\theta}_{F,i\sigma}\int d^3r_1d^3r_2\psi_{i\sigma}^*(\mathbf{r}_1)K(\mathbf{r};\mathbf{r}_1,\mathbf{r}_2)\psi_{i\sigma}(\mathbf{r}_2)=\sum_i\tilde{\theta}_{F,i\sigma}\langle\psi_{i\sigma}|K(\mathbf{r})|\psi_{i\sigma}\rangle, \quad (4)$$

where, following Ref. 8, I introduced a compact notation $\tilde{\theta}_{F,i\sigma}=\tilde{\theta}[(\varepsilon_F-\varepsilon_{i\sigma})/\eta]$. With a NC PP, the electron valence charge densities of the noninteracting auxiliary electron system (and hence of the interacting one) are the sum of the square moduli of the wave functions, weighted by the occupation numbers. In the present scheme, this case is recovered by taking $K(\mathbf{r};\mathbf{r}_1,\mathbf{r}_2)=\delta(\mathbf{r}-\mathbf{r}_1)\delta(\mathbf{r}-\mathbf{r}_2)$. In the US PP's scheme the function $K(\mathbf{r};\mathbf{r}_1,\mathbf{r}_2)$ contains an augmentation term (I refer to Refs. 18 and 32 for additional details):

$$K(\mathbf{r};\mathbf{r}_1,\mathbf{r}_2)=\delta(\mathbf{r}-\mathbf{r}_1)\,\delta(\mathbf{r}-\mathbf{r}_2)+\sum_{Inm} Q_{nm}^{\gamma(I)}(\mathbf{r}-\mathbf{R}_I) \times\beta_n^{\gamma(I)}(\mathbf{r}_1-\mathbf{R}_I)\beta_m^{*\gamma(I)}(\mathbf{r}_2-\mathbf{R}_I). \quad (5)$$

The augmentation functions $Q_{nm}^{\gamma(I)}(\mathbf{r}-\mathbf{R}_I)$ are calculated together with the PP and are localized about the atoms. When the atoms move, the centers of the augmentation functions change. Therefore, to develop a perturbation scheme, we must consider $K(\mathbf{r};\mathbf{r}_1,\mathbf{r}_2)$ as a function of the perturbation parameters. F is the sum of the local, Hartree, and exchange and correlation energies:

$$F[\rho_\sigma(\mathbf{r}),\rho_{c,\sigma}(\mathbf{r})]=\int d^3r V_{loc}(\mathbf{r})\rho(\mathbf{r})+\frac{1}{2}\int d^3r_1 d^3r_2 \times\frac{\rho(\mathbf{r}_1)\rho(\mathbf{r}_2)}{|\mathbf{r}_1-\mathbf{r}_2|}+E_{xc}[n_\sigma(\mathbf{r}),\nabla n_\sigma(\mathbf{r})], \quad (6)$$

where the total valence charge $\rho(\mathbf{r})$ is the sum of the spin-up and spin-down valence electron densities, $\rho_{c,\sigma}(\mathbf{r})$ are the core charges obtained from the atomic core charges, and $n_\sigma(\mathbf{r})=\rho_\sigma(\mathbf{r})+\rho_{c,\sigma}(\mathbf{r})$ are the total spin charge densities. $V_{loc}(\mathbf{r})=\Sigma_I V_{loc}^{\gamma(I)}(\mathbf{r}-\mathbf{R}_I)$ is the local part of the PP. E_{xc} is the exchange and correlation energy functional. Following the NLCC recipe, I assume that E_{xc} is a functional of the total spin charge densities. In GGA, E_{xc} depends also on the gradients, $\nabla n_\sigma(\mathbf{r})$. Core spin polarization is neglected, assuming that $\rho_{c,\sigma}(\mathbf{r})=1/2\rho_c(\mathbf{r})$. The core charge does not depend on the orbitals but it is a function of the atomic positions.

The term U_{II}, in Eq. (1), is the ion-ion interaction dealt with via the Ewald summation method. In the following, I focus only on the electronic contribution to the force constants. The ionic contribution is discussed in several papers[2,7,33] and no new feature is introduced by the US PP's scheme.

The last term in the energy functional, Eq. (1), is a correction that resembles an entropy term for fixed electron numbers and is nonvanishing for fractional occupation numbers. It coincides with an entropy term when the occupation factors have the Fermi-Dirac form. In this case F_{tot} is a free-energy functional. In general, the function $\tilde{\theta}_1(x)$ is: $\tilde{\theta}_1(x)=\int_{-\infty}^{x} y\tilde{\delta}(y)dy$. With this definition, the energy in Eq. (1) is variational and is equivalent to the energy introduced for instance in Ref. 29, as discussed in Refs. 2 and 8. It is equivalent to assume that the occupation numbers are independent parameters, as in Ref. 29, and to use the variational energy to determine them, or to treat them as a function of the single-particle energies as done here. In the latter case, the minimization of the energy yields the KS equations for the orbitals and, in the formulas for the HF forces, the occupation numbers derivatives do not appear.[28,8] This formalism, which reduces to the finite temperature DFT with Fermi-Dirac occupation factors, is used in this paper in the context of the smearing approach to metals and its main purpose is the efficient evaluation of BZ integrals in the presence of a Fermi surface.

The orbitals $\{\psi_{i\sigma}(\mathbf{r})\}$ are subject to generalized orthonormalization constraints:[18]

$$\langle\psi_{i\sigma}|S|\psi_{j\sigma}\rangle=\delta_{ij}, \quad (7)$$

with an overlap matrix S:

$$S(\mathbf{r}_1,\mathbf{r}_2)=\delta(\mathbf{r}_1-\mathbf{r}_2) +\sum_{Inm} q_{nm}^{\gamma(I)}\beta_n^{\gamma(I)}(\mathbf{r}_1-\mathbf{R}_I)\beta_m^{*\gamma(I)}(\mathbf{r}_2-\mathbf{R}_I), \quad (8)$$

where the coefficients $q_{nm}^{\gamma(I)}=\int d^3r Q_{nm}^{\gamma(I)}(\mathbf{r})$ are the integrals of the augmentation functions. Given this definition of S, the charge conservation condition in the US PP's scheme becomes identical to the one found in the NC scheme. This condition defines the Fermi energy and it is

$$\sum_{i\sigma}\tilde{\theta}_{F,i\sigma}=N_{el}. \quad (9)$$

The ground-state spin charge densities minimize the energy functional. As a consequence, the KS functional is minimized by the auxiliary single-particle orbitals $\{\psi_{i\sigma}(\mathbf{r})\}$. With the constraints in Eq. (7), the minimum condition leads to the KS equations:

$$\left[-\frac{1}{2}\nabla^2+V_{NL}+\int d^3r V_{eff}^{\sigma}(\mathbf{r})K(\mathbf{r})\right]|\psi_{l\sigma}\rangle=\varepsilon_{l\sigma}S|\psi_{l\sigma}\rangle, \quad (10)$$

where the effective potential is the sum of the local, Hartree, and exchange and correlation potentials:

$$V_{eff}^{\sigma}(\mathbf{r})=\frac{\partial F}{\partial\rho_\sigma(\mathbf{r})}=V_{loc}(\mathbf{r})+\int d^3r_1\frac{\rho(\mathbf{r}_1)}{|\mathbf{r}-\mathbf{r}_1|}+V_{xc}^{\sigma}(\mathbf{r}). \quad (11)$$

The expression of $V_{xc}^{\sigma}(\mathbf{r})$, in the context of the GGA approximation, is given in Ref. 22. To simplify the notation, the KS potential is defined as

$$V_{KS}^{\sigma}(\mathbf{r}_1,\mathbf{r}_2)=V_{NL}(\mathbf{r}_1,\mathbf{r}_2)+\int d^3r V_{eff}^{\sigma}(\mathbf{r})K(\mathbf{r};\mathbf{r}_1,\mathbf{r}_2). \quad (12)$$

At the electronic ground state, the forces acting on the atoms are the negative derivatives of the energy functional [Eq. (1)] with respect to atomic displacements. The atomic positions act as external parameters in this functional thus the HF theorem[6] applies: the forces depend only on the ground-state orbitals. In the US PP's scheme, the overlap matrix S changes as the atoms move, thus giving rise to a

term in the forces. This term is found using the linearized orthonormalization constraints which provide the relationships

$$\left\langle \frac{d\psi_{i\sigma}}{d\lambda}\middle| S|\psi_{j\sigma}\right\rangle + \langle \psi_{i\sigma}|S\left|\frac{d\psi_{j\sigma}}{d\lambda}\right\rangle = -\langle \psi_{i\sigma}|\frac{\partial S}{\partial \lambda}|\psi_{j\sigma}\rangle, \quad (13)$$

where λ denotes the amplitude of an atomic displacement. The final expression of the energy derivative is

$$\frac{dF_{tot}}{d\lambda} = \sum_{i\sigma} \tilde{\theta}_{F,i\sigma}\langle \psi_{i\sigma}|\frac{\partial V^{\sigma}_{KS}}{\partial \lambda} - \varepsilon_{i\sigma}\frac{\partial S}{\partial \lambda}|\psi_{i\sigma}\rangle + \sum_{\sigma}\int d^3r_1 V^{\sigma}_{xc}(\mathbf{r}_1)\frac{\partial \rho_{c,\sigma}(\mathbf{r}_1)}{\partial \lambda}, \quad (14)$$

where the last term accounts for the NLCC, and the partial derivative of V^{σ}_{KS} is defined as

$$\frac{\partial V^{\sigma}_{KS}(\mathbf{r}_1,\mathbf{r}_2)}{\partial \lambda} = \frac{\partial V_{NL}(\mathbf{r}_1,\mathbf{r}_2)}{\partial \lambda} + \int d^3r \frac{\partial V_{loc}(\mathbf{r})}{\partial \lambda}K(\mathbf{r};\mathbf{r}_1,\mathbf{r}_2) + \int d^3r V^{\sigma}_{eff}(\mathbf{r})\frac{\partial K(\mathbf{r};\mathbf{r}_1,\mathbf{r}_2)}{\partial \lambda}. \quad (15)$$

In these expressions and in the following, I use the total derivative symbol (d) to denote a derivative where the orbitals are considered as implicit functions of λ, while the partial derivative symbol (∂) indicates derivatives done at fixed orbitals. The partial derivative is used also to differentiate quantities such as S or ρ_c which do not depend on the orbitals. For fixed occupation numbers and neglecting NLCC, Eq. (14) has been reported in several papers (see, for instance, Ref. 32). In order to calculate the interatomic force constants and hence the dynamical matrix, I differentiate Eq. (14) with respect to a second perturbation parameter μ. $dF_{tot}/d\lambda$ does not depend either on the induced spin charge densities or on the first-order wave-function derivatives with respect to λ. Therefore the mixed second-order energy derivatives will depend only on the induced spin charge densities and on the first-order change in the orbitals with respect to μ. Before differentiating Eq. (14), in the next section, I discuss how to calculate the induced charge-density and the wave-function changes within the US PP's scheme.

III. FIRST-ORDER WAVE-FUNCTION AND CHARGE-DENSITY DERIVATIVES

The spin-up and spin-down charge densities are calculated via Eq. (4). By differentiating this expression with respect to the perturbation parameter μ, I get the induced spin charge densities at first order. There are three terms. The first one is the spin charge density induced by the change in the occupation factors:

$$\frac{d\rho^{(a)}_{\sigma}(\mathbf{r})}{d\mu} = \sum_i \frac{d\tilde{\theta}_{F,i\sigma}}{d\mu}\langle \psi_{i\sigma}|K(\mathbf{r})|\psi_{i\sigma}\rangle, \quad (16)$$

while the second one accounts for the change in the wave functions:

$$\frac{d\rho^{(b)}_{\sigma}(\mathbf{r})}{d\mu} = \sum_i \tilde{\theta}_{F,i\sigma}\left[\left\langle \frac{d\psi_{i\sigma}}{d\mu}\middle| K(\mathbf{r})|\psi_{i\sigma}\right\rangle + \text{c.c.}\right], \quad (17)$$

where c.c. indicates the complex conjugate. The third term has no correspondent counterpart in the NC scheme. It is due to the displacement of the augmentation functions and it is written

$$\frac{d\rho^{(c)}_{\sigma}(\mathbf{r})}{d\mu} = \sum_i \tilde{\theta}_{F,i\sigma}\langle \psi_{i\sigma}|\frac{\partial K(\mathbf{r})}{\partial \mu}|\psi_{i\sigma}\rangle. \quad (18)$$

Two new quantities appear in Eqs. (16) and (17): the variation of the occupation numbers and the first-order change in the wave functions. In insulators and with NC PP's, one can show that only the conduction-band projection of $|d\psi_{i\sigma}/d\mu\rangle$ contributes to the induced spin charge density and, of course, the occupation numbers are fixed. As shown in Ref. 8, in metals one can define a generalized projector in the conduction-band manifold and set up a linear system to get the wave-function changes, in such a way that Eqs. (16) and (17) are calculated with expressions which closely resemble those valid for insulators. With respect to Ref. 8, the major difficulty of the US PP's scheme originates from the dependence of S, and hence of the orthonormalization constraints, on the atomic positions. By contrast, the displacement of the augmentation functions gives rise to Eq. (18) which can be calculated as it is, without further manipulations.

First-order perturbation theory, applied to the KS equations [Eq. (10)], yields the components of $|d\psi_{i\sigma}/d\mu\rangle$ in the subspace orthogonal to the eigenspace of $|\psi_{i\sigma}\rangle$ and also the energy levels derivatives with respect to μ. Differentiation of Eq. (10) yields

$$\left[-\frac{1}{2}\nabla^2 + V^{\sigma}_{KS} - \varepsilon_{i\sigma}S\right]\left|\frac{d\psi_{i\sigma}}{d\mu}\right\rangle = -\left[\frac{dV^{\sigma}_{KS}}{d\mu} - \varepsilon_{i\sigma}\frac{\partial S}{\partial \mu}\right]|\psi_{i\sigma}\rangle + \frac{d\varepsilon_{i\sigma}}{d\mu}S|\psi_{i\sigma}\rangle, \quad (19)$$

where the total derivative of the KS potential is

$$\frac{dV^{\sigma}_{KS}(\mathbf{r}_1,\mathbf{r}_2)}{d\mu} = \frac{\partial V^{\sigma}_{KS}(\mathbf{r}_1,\mathbf{r}_2)}{\partial \mu} + \int d^3r \frac{dV^{\sigma}_{Hxc}(\mathbf{r})}{d\mu}K(\mathbf{r};\mathbf{r}_1,\mathbf{r}_2). \quad (20)$$

This derivative differs from the partial derivative of $V^{\sigma}_{KS}(\mathbf{r}_1,\mathbf{r}_2)$, discussed above [see Eq. (15)], for the presence of a self-consistent term. Indeed, $dV^{\sigma}_{Hxc}(\mathbf{r})/d\mu$ is the change in the Hartree and exchange and correlation potential:

$$\frac{dV^{\sigma}_{Hxc}(\mathbf{r})}{d\mu} = \int d^3r_1 \frac{d\rho(\mathbf{r}_1)}{d\mu}\frac{1}{|\mathbf{r}-\mathbf{r}_1|} + \frac{dV^{\sigma}_{xc}(\mathbf{r})}{d\mu}, \quad (21)$$

linear in the induced spin charge densities. $dV^{\sigma}_{xc}(\mathbf{r})/d\mu$, in the GGA approximation, is calculated in Ref. 22.

The linear system in Eq. (19) is singular as in the NC case where, in order to solve it, one projects both sides in the conduction-band manifold and adds to the left-hand side a multiple of the valence-band projector so as to make the

system nonsingular.[2] In the NC case, the solutions of the projected linear system suffice since only the conduction-band projection of $|d\psi_{i\sigma}/d\mu\rangle$ contributes to the induced spin charge densities and to the interatomic force constants. In the US case, instead, also the valence-band projection of $|d\psi_{i\sigma}/d\mu\rangle$ gives a finite contribution to $d\rho_\sigma(\mathbf{r})/d\mu$ since S is changing with the perturbation. In the following, I show how this works in the US PP's scheme. As shown in Ref. 8, one can deal with the general case of metals, insulators are a special case. I assume that $\varepsilon_{i\sigma}$ is nondegenerate, but the generalization to the degenerate case is straightforward. Projecting Eq. (19) on the unperturbed orbitals $\{|\psi_{i\sigma}\rangle\}$ gives

$$\frac{d\varepsilon_{i\sigma}}{d\mu}=\langle\psi_{i\sigma}|\left[\frac{dV_{KS}^{\sigma}}{d\mu}-\varepsilon_{i\sigma}\frac{\partial S}{\partial\mu}\right]|\psi_{i\sigma}\rangle, \tag{22}$$

and for $j\neq i$:

$$\langle\psi_{j\sigma}|S\left|\frac{d\psi_{i\sigma}}{d\mu}\right\rangle=\frac{\langle\psi_{j\sigma}|\left[\frac{dV_{KS}^{\sigma}}{d\mu}-\varepsilon_{i\sigma}\frac{\partial S}{\partial\mu}\right]|\psi_{i\sigma}\rangle}{\varepsilon_{i\sigma}-\varepsilon_{j\sigma}}. \tag{23}$$

Using Eq. (23), the transformation discussed in Ref. 8, and additional bookkeeping to account for the energy-level exchanges, Eq. (17) can be rewritten as

$$\frac{d\rho_\sigma^{(b)}(\mathbf{r})}{d\mu}=2\,\mathrm{Re}\left\{\sum_i\sum_{j\neq i}\frac{\tilde{\theta}_{F,i\sigma}-\tilde{\theta}_{F,j\sigma}}{\varepsilon_{i\sigma}-\varepsilon_{j\sigma}}\theta_{j\sigma,i\sigma}\rho_{i\sigma,j\sigma}\langle\psi_{j\sigma}|\left[\frac{dV_{KS}^{\sigma}}{d\mu}-\varepsilon_{i\sigma}\frac{\partial S}{\partial\mu}\right]|\psi_{i\sigma}\rangle\right\}$$
$$-\sum_i\sum_j\left[\tilde{\theta}_{F,i\sigma}\theta_{i\sigma,j\sigma}+\tilde{\theta}_{F,j\sigma}\theta_{j\sigma,i\sigma}\right]\rho_{i\sigma,j\sigma}\langle\psi_{j\sigma}|\frac{\partial S}{\partial\mu}|\psi_{i\sigma}\rangle, \tag{24}$$

where $\rho_{i\sigma,j\sigma}=\langle\psi_{i\sigma}|K(\mathbf{r})|\psi_{j\sigma}\rangle$, and θ is a step function. In the first term of Eq. (24) the $j=i$ term is missing. In a metal, the change in the occupation numbers could give rise to a nonvanishing $j=i$ term. In fact, Eq. (16) can be split as

$$\frac{d\rho_\sigma^{(a)}(\mathbf{r})}{d\mu}=\sum_i\frac{d\tilde{\theta}_{F,i\sigma}}{d\mu}\rho_{i\sigma,i\sigma}$$
$$=\sum_i\frac{1}{\eta}\tilde{\delta}_{F,i\sigma}\frac{d\varepsilon_F}{d\mu}\rho_{i\sigma,i\sigma}-\sum_i\frac{1}{\eta}\tilde{\delta}_{F,i\sigma}\frac{d\varepsilon_{i\sigma}}{d\mu}\rho_{i\sigma,i\sigma}. \tag{25}$$

In the limit $\varepsilon_{j\sigma}\to\varepsilon_{i\sigma}$, the ratio $(\tilde{\theta}_{F,i\sigma}-\tilde{\theta}_{F,j\sigma})/(\varepsilon_{i\sigma}-\varepsilon_{j\sigma})$ is equal to $-(1/\eta)\tilde{\delta}_{F,i\sigma}$. Therefore the second term in Eq. (25) is the missing $j=i$ term of Eq. (24) and can be included in the sum. The first term of Eq. (25) shows that the change in the Fermi energy could affect the induced spin charge densities (see Ref. 2 for a discussion of the origin of this term). Equation (24) is a central result of this paper. The last term shows how the changing orthonormalization constraints affect the induced charge densities and how the variable occupation numbers must be handled.

To proceed further, let us define two vectors:

$$|\Delta^\mu\psi_{i\sigma}\rangle=\frac{1}{2\eta}\tilde{\delta}_{F,i\sigma}\frac{d\varepsilon_F}{d\mu}|\psi_{i\sigma}\rangle+\sum_j\frac{\tilde{\theta}_{F,i\sigma}-\tilde{\theta}_{F,j\sigma}}{\varepsilon_{i\sigma}-\varepsilon_{j\sigma}}\theta_{j\sigma,i\sigma}|\psi_{j\sigma}\rangle$$
$$\times\langle\psi_{j\sigma}|\left[\frac{dV_{KS}^{\sigma}}{d\mu}-\varepsilon_{i\sigma}\frac{\partial S}{\partial\mu}\right]|\psi_{i\sigma}\rangle \tag{26}$$

and

$$|\delta^\mu\psi_{i\sigma}\rangle=\sum_j\left[\tilde{\theta}_{F,i\sigma}\theta_{i\sigma,j\sigma}+\tilde{\theta}_{F,j\sigma}\theta_{j\sigma,i\sigma}\right]|\psi_{j\sigma}\rangle\langle\psi_{j\sigma}|\frac{\partial S}{\partial\mu}|\psi_{i\sigma}\rangle. \tag{27}$$

In an insulator, $|\Delta^\mu\psi_{i\sigma}\rangle$ is the projection of $|d\psi_{i\sigma}/d\mu\rangle$ on the conduction-band manifold, while $|\delta^\mu\psi_{i\sigma}\rangle$ is reminiscent of a projection of $|d\psi_{i\sigma}/d\mu\rangle$ in the valence-band manifold. It is nonvanishing only if the orthonormalization constraints are variable. Given these definitions, at linear order, the induced spin charge densities become

$$\frac{d\rho_\sigma(\mathbf{r})}{d\mu}=2\,\mathrm{Re}\sum_i\langle\psi_{i\sigma}|K(\mathbf{r})|\Delta^\mu\psi_{i\sigma}\rangle-\sum_i\langle\psi_{i\sigma}|$$
$$\times K(\mathbf{r})|\delta^\mu\psi_{i\sigma}\rangle+\sum_i\tilde{\theta}_{F,i\sigma}\langle\psi_{i\sigma}|\frac{\partial K(\mathbf{r})}{\partial\mu}|\psi_{i\sigma}\rangle. \tag{28}$$

Equation (28), limited to spin unpolarized insulators, has been presented in Ref. 19. As in Ref. 19, in the following, the last two terms are called $\Delta^\mu\rho_\sigma(\mathbf{r})$, while the second term is called $\delta^\mu\rho_{\sigma,orth}(\mathbf{r})$.

IV. LINEAR SYSTEM

The sum over j in the definition of the vector $|\delta^\mu\psi_{i\sigma}\rangle$ [Eq. (27)] is over all states, but actually the $\tilde{\theta}$ functions limit the sum to filled and partially filled states. We can assume that $\tilde{\theta}_{F,j\sigma}$ is vanishing if the eigenvalue $\varepsilon_{j\sigma}$ is higher than $\varepsilon_F+3\eta$. Instead the sum over j, in the definition of $|\Delta^\mu\psi_{i\sigma}\rangle$ [Eq. (26)], extends to all states. In principle this is an infinite sum. If the orbitals are expanded in a finite basis set, the sum is over a number of states comparable to the number of basis functions. The explicit evaluation of $|\Delta^\mu\psi_{i\sigma}\rangle$ via Eq. (26) is computationally expensive since it requires the knowledge of

all the eigenvectors of Eq. (10) and summations over all states. Instead, the sum can be carried out exactly and efficiently by solving an algebraic linear system. This formalism is known as the Green-function technique.[1] I introduce a linear system whose solution is $|\tilde{\Delta}^{\mu}\psi_{i\sigma}\rangle = |\Delta^{\mu}\psi_{i\sigma}\rangle - (1/2\,\eta)\tilde{\delta}_{F,i\sigma}(d\varepsilon_F/d\mu)|\psi_{i\sigma}\rangle$. Following Ref. 8:

$$\left[-\frac{1}{2}\nabla^2 + V_{KS}^{\sigma} + Q^{\sigma} - \varepsilon_{i\sigma}S\right]|\tilde{\Delta}^{\mu}\psi_{i\sigma}\rangle = -P_{c,i\sigma}^{\dagger}\left[\frac{dV_{KS}^{\sigma}}{d\mu} - \varepsilon_{i\sigma}\frac{\partial S}{\partial \mu}\right]|\psi_{i\sigma}\rangle, \tag{29}$$

with

$$P_{c,i\sigma}^{\dagger} = \left[\tilde{\theta}_{F,i\sigma} - \sum_j \beta_{i\sigma,j\sigma}S|\psi_{j\sigma}\rangle\langle\psi_{j\sigma}|\right]. \tag{30}$$

Q^{σ} is an operator, vanishing on the conduction states above $\varepsilon_F + 3\,\eta$, which makes the linear system nonsingular. In the US PP's scheme it is: $Q^{\sigma} = \Sigma_j \alpha_{j\sigma}S|\psi_{j\sigma}\rangle\langle\psi_{j\sigma}|S$, where $\alpha_{j\sigma}$ is vanishing if $\varepsilon_{j\sigma}$ is above $\varepsilon_F + 3\,\eta$ and is equal to $\varepsilon_F + 3\,\eta - \varepsilon_{j\sigma}$ if it is below. This linear system can be solved with iterative techniques, such as the conjugate gradient method. By projecting on the unperturbed levels, one shows that by choosing the $\beta_{i\sigma,j\sigma}$ as

$$\beta_{i\sigma,j\sigma} = \tilde{\theta}_{F,i\sigma}\theta_{i\sigma,j\sigma} + \tilde{\theta}_{F,j\sigma}\theta_{j\sigma,i\sigma} + \alpha_{j\sigma}\frac{\tilde{\theta}_{F,i\sigma} - \tilde{\theta}_{F,j\sigma}}{\varepsilon_{i\sigma} - \varepsilon_{j\sigma}}\theta_{j\sigma,i\sigma}, \tag{31}$$

its solution is indeed the vector $|\tilde{\Delta}^{\mu}\psi_{i\sigma}\rangle$ [see Eq. (26)]. Note that with this definition all sums are limited to states with energy lower than $\varepsilon_F + 3\,\eta$. In insulators $\tilde{\theta}_{F,i\sigma} - \Sigma_j \beta_{i\sigma,j\sigma}S|\psi_{j\sigma}\rangle\langle\psi_{j\sigma}|$ becomes the projector over the conduction states manifold $P_c^{\dagger}$, which does not depend on the energy level. For nonmagnetic and insulating solids, this linear system [Eq. (29)] was introduced in Ref. 19.

V. MIXED SECOND-ORDER ENERGY DERIVATIVES

In this section I calculate the mixed second-order energy derivatives with respect to atomic displacements. Differentiation of Eq. (14) with respect to μ gives four terms. The first accounts for the change in the occupation numbers:

$$\frac{d^2F_{tot}^{(a)}}{d\mu d\lambda} = \sum_{i\sigma} \frac{d\tilde{\theta}_{F,i\sigma}}{d\mu}\langle\psi_{i\sigma}|\left[\frac{\partial V_{KS}^{\sigma}}{\partial\lambda} - \varepsilon_{i\sigma}\frac{\partial S}{\partial\lambda}\right]|\psi_{i\sigma}\rangle. \tag{32}$$

The second is due to the change in the energy levels and in the wave functions:

$$\frac{d^2F_{tot}^{(b)}}{d\mu d\lambda} = -\sum_{i\sigma} \tilde{\theta}_{F,i\sigma}\frac{d\varepsilon_{i\sigma}}{d\mu}\langle\psi_{i\sigma}|\frac{\partial S}{\partial\lambda}|\psi_{i\sigma}\rangle + \sum_{i\sigma} \tilde{\theta}_{F,i\sigma}\left\{\left\langle\frac{d\psi_{i\sigma}}{d\mu}\right|\left[\frac{\partial V_{KS}^{\sigma}}{\partial\lambda} - \varepsilon_{i\sigma}\frac{\partial S}{\partial\lambda}\right]|\psi_{i\sigma}\rangle + \text{c.c.}\right\}. \tag{33}$$

The third term generalizes to the US PP's scheme, the expectation value of the mixed second-order derivative of the external potential:

$$\frac{d^2F_{tot}^{(c)}}{d\mu d\lambda} = \sum_{i\sigma} \tilde{\theta}_{F,i\sigma}\langle\psi_{i\sigma}|\left[\frac{d}{d\mu}\left(\frac{\partial V_{KS}^{\sigma}}{\partial\lambda}\right) - \varepsilon_{i\sigma}\frac{\partial^2 S}{\partial\mu\partial\lambda}\right]|\psi_{i\sigma}\rangle. \tag{34}$$

The fourth term is due to NLCC and is equal to Eqs. (134) and (135) of Ref. 2 (see also Ref. 34):

$$\frac{d^2F_{tot}^{(d)}}{d\mu d\lambda} = \sum_{\sigma}\int d^3r_1 \frac{dV_{xc}^{\sigma}(\mathbf{r}_1)}{d\mu}\frac{\partial\rho_{c,\sigma}(\mathbf{r}_1)}{\partial\lambda} + \sum_{\sigma}\int d^3r_1 V_{xc}^{\sigma}(\mathbf{r}_1)\frac{\partial^2\rho_{c,\sigma}(\mathbf{r}_1)}{\partial\mu\partial\lambda}. \tag{35}$$

The two vectors $|\Delta^{\mu}\psi_{i\sigma}\rangle$, and $|\delta^{\mu}\psi_{i\sigma}\rangle$ introduced to calculate the induced spin charge densities suffice also to evaluate the mixed second-order energy derivatives. I start with Eq. (33). Using Eqs. (22) and (23) for the change in the energy levels and in the wave functions and techniques similar to those applied to derive Eq. (24), one transforms Eq. (33) into

$$\frac{d^2F_{tot}^{(b)}}{d\mu d\lambda} = 2\,\text{Re}\left\{\sum_{i\sigma}\sum_{j\neq i}\frac{\tilde{\theta}_{F,i\sigma} - \tilde{\theta}_{F,j\sigma}}{\varepsilon_{i\sigma} - \varepsilon_{j\sigma}}\theta_{j\sigma,i\sigma}\langle\psi_{i\sigma}|\left[\frac{dV_{KS}^{\sigma}}{d\mu} - \varepsilon_{i\sigma}\frac{\partial S}{\partial\mu}\right]|\psi_{j\sigma}\rangle\langle\psi_{j\sigma}|\left[\frac{\partial V_{KS}^{\sigma}}{\partial\lambda} - \varepsilon_{i\sigma}\frac{\partial S}{\partial\lambda}\right]|\psi_{i\sigma}\rangle\right\}$$
$$-\sum_{i\sigma}\sum_{j}\left\{[\tilde{\theta}_{F,i\sigma}\theta_{i\sigma,j\sigma} + \tilde{\theta}_{F,j\sigma}\theta_{j\sigma,i\sigma}]\langle\psi_{i\sigma}|\frac{\partial S}{\partial\mu}|\psi_{j\sigma}\rangle\langle\psi_{j\sigma}|\left[\frac{\partial V_{KS}^{\sigma}}{\partial\lambda} - \varepsilon_{i\sigma}\frac{\partial S}{\partial\lambda}\right]|\psi_{i\sigma}\rangle + (\mu\leftrightarrow\lambda)\right\}$$
$$+\sum_{\sigma}\int d^3r\frac{dV_{Hxc}^{\sigma}(\mathbf{r})}{d\mu}\delta^{\lambda}\rho_{\sigma,orth}(\mathbf{r}), \tag{36}$$

where $(\mu \leftrightarrow \lambda)$ denotes a term equal to the one in the bracket, with λ exchanged with μ. Equation (36) is the second main result of this paper. It shows how the change in the orthonormalization constraints reflects in the expression of the interatomic force constants and how to handle partial occupations. Furthermore, it shows that $\delta^{\lambda}\rho_{\sigma,orth}(\mathbf{r})$ couples with the variation of $V^{\sigma}_{Hxc}(\mathbf{r})$.

Equation (32) is transformed as Eq. (16). It is split into the missing $j=i$ term of Eq. (36) and into a contribution due to the Fermi energy change.

In the NC case, the expectation value of the mixed second-order derivatives of the electron-ion potential is formally similar to Eq. (34). However, this equation differs from the NC case since the augmentation functions make $\partial V^{\sigma}_{KS}/\partial\lambda$ dependent on the charge densities through V^{σ}_{eff} [see Eq. (15)] and therefore the μ derivative of $\partial V^{\sigma}_{KS}/\partial\lambda$ depends also on the induced self-consistent charge densities. Expanding the total derivative with respect to μ one obtains

$$\frac{d}{d\mu}\left(\frac{\partial V^{\sigma}_{KS}}{\partial\lambda}\right)=\frac{\partial^2 V^{\sigma}_{KS}}{\partial\mu\partial\lambda}+\int d^3r\frac{dV^{\sigma}_{Hxc}(\mathbf{r})}{d\mu}\frac{\partial K(\mathbf{r})}{\partial\lambda}, \tag{37}$$

where the mixed partial derivative of V^{σ}_{KS} is

$$\begin{aligned}\frac{\partial^2 V^{\sigma}_{KS}(\mathbf{r}_1,\mathbf{r}_2)}{\partial\mu\partial\lambda}=&\frac{\partial^2 V_{NL}(\mathbf{r}_1,\mathbf{r}_2)}{\partial\mu\partial\lambda}+\int d^3r\frac{\partial^2 V_{loc}(\mathbf{r})}{\partial\mu\partial\lambda}K(\mathbf{r};\mathbf{r}_1,\mathbf{r}_2)\\&+\int d^3r V^{\sigma}_{eff}(\mathbf{r})\frac{\partial^2 K(\mathbf{r};\mathbf{r}_1,\mathbf{r}_2)}{\partial\mu\partial\lambda}\\&+\left[\int d^3r\frac{\partial V_{loc}(\mathbf{r})}{\partial\lambda}\frac{\partial K(\mathbf{r};\mathbf{r}_1,\mathbf{r}_2)}{\partial\mu}+(\lambda\leftrightarrow\mu)\right].\end{aligned} \tag{38}$$

Collecting these results [Eqs. (36)–(38)], and ordering the terms as in Ref. 19, the mixed second-order energy derivatives assume the final form. The first two terms generalize, to the US case, the NC terms in the interatomic force constants. The expectation value of the second derivative of the electron-ion potential becomes

$$\frac{d^2F^{(1)}_{tot}}{d\mu d\lambda}=\sum_{i\sigma}\tilde{\theta}_{F,i\sigma}\langle\psi_{i\sigma}|\left[\frac{\partial^2 V^{\sigma}_{KS}}{\partial\mu\partial\lambda}-\varepsilon_{i\sigma}\frac{\partial^2 S}{\partial\mu\partial\lambda}\right]|\psi_{i\sigma}\rangle, \tag{39}$$

and the change in the wave functions gives a term

$$\frac{d^2F^{(2)}_{tot}}{d\mu d\lambda}=2\,\mathrm{Re}\sum_{i\sigma}\langle\Delta^{\mu}\psi_{i\sigma}|\left[\frac{\partial V^{\sigma}_{KS}}{\partial\lambda}-\varepsilon_{i\sigma}\frac{\partial S}{\partial\lambda}\right]|\psi_{i\sigma}\rangle. \tag{40}$$

In the US PP's scheme one must consider two additional contributions, which have no correspondent counterparts in the NC scheme. The first is the interaction between the change in V^{σ}_{Hxc} and $\Delta^{\lambda}\rho_{\sigma}$:

$$\frac{d^2F^{(3)}_{tot}}{d\mu d\lambda}=\sum_{\sigma}\int d^3r\frac{dV^{\sigma}_{Hxc}(\mathbf{r})}{d\mu}\Delta^{\lambda}\rho_{\sigma}(\mathbf{r}). \tag{41}$$

$\Delta^{\lambda}\rho_{\sigma}$ includes both the orthonormalization term, $\delta^{\lambda}\rho_{\sigma,orth}$, and the charge induced by the displacement of the augmentation functions [Eq. (18)]. This integral is obtained partially in Eq. (37), from the μ derivative of $\partial V^{\sigma}_{KS}/\partial\lambda$, and partially in Eq. (36) from the manipulation of $d^2F^{(b)}_{tot}/d\mu d\lambda$

The fourth term, obtained in Eq. (36), has the same origin as $\delta^{\lambda}\rho_{\sigma,orth}$, it is due to the dependence of the orthonormalization constraints on the atomic positions:

$$\frac{d^2F^{(4)}_{tot}}{d\mu d\lambda}=-\sum_{i\sigma}\left\{\langle\delta^{\mu}\psi_{i\sigma}|\left[\frac{\partial V^{\sigma}_{KS}}{\partial\lambda}-\varepsilon_{i\sigma}\frac{\partial S}{\partial\lambda}\right]|\psi_{i\sigma}\rangle+(\mu\leftrightarrow\lambda)\right\}. \tag{42}$$

For nonmagnetic, insulating materials these terms have been discussed in Ref. 19 and in Ref. 2. Equation (35) accounts for NLCC and is added to these four terms.[2,34] In Appendix A, I shall show how to exploit these relationships to get the dynamical matrices of a periodic solid.

VI. PHONON DISPERSIONS OF CU(001)

In this section the vibrational properties of the Cu(001) surface are investigated by DFPT with US PP's. The surface is simulated by 39 and 107 layer slabs.[38] The interatomic force constants of these slabs are calculated from the bulk Cu and from a seven layer Cu(001) slab. The latter provides the interactions among three surface layers whereas the former describes the force constants in the other layers. The exchange and correlation energy functional is approximated by the LDA (Ref. 27) or by the Perdew, Burke, and Ernzerhof (PBE) (Ref. 35) GGA. The phonon dispersions obtained with these two functionals are compared. A similar comparison was carried out for bulk Cu in Ref. 21. In this work, I use the same Cu PP's. PW's up to a cutoff of 25 (30) Ry for the wave functions and 200 (480) Ry for the charge density are included in the basis set in the LDA (PBE GGA).

The seven layer slab is studied with a tetragonal unit cell. The periodically repeated slabs are separated by a vacuum space equivalent to eight (LDA) and nine (PBE GGA) layers. The in-plane lattice constant is $a_0=6.71$ a.u. (LDA), and $a_0=6.95$ a.u. (PBE GGA) which are the theoretical values in the bulk. **k**-point sampling is done with 21 points in the irreducible wedge of the surface BZ (SBZ). The smearing parameter is $\eta=0.05$ Ry. The interlayer spacings are relaxed, starting from the ideal surface and minimizing the energy. At equilibrium, the forces acting on the atoms are less than 0.2 mRy/a.u.. The relaxation is mainly confined to the first layer which relaxes inward, $d_{12}=-3.0\%$ both in LDA and in PBE GGA. The second and third layers do not relax appreciably. A more detailed account of the calculated geometrical parameters of the Cu(001) surface can be found in Ref. 23.

The dynamical matrices of the seven layer slab are evaluated via Eqs. (B32)–(B37) on a 4×4 mesh of **q** points in the SBZ. A Fourier transform of these matrices provides the interatomic force constants of three surface layers, until five neighbors on the surface. A frozen phonon calculation of comparable accuracy would require 16 surface atoms (the unit cell would contain 106 atoms). Table I presents a comparison of the interatomic force constants obtained at the surface and within the bulk. The interactions of a Cu atom with its first neighbor on the surface and with the first neigh-

TABLE I. Theoretical LDA and PBE GGA interatomic force constants of the Cu(001) surface. The moving atom is at the origin, whereas the coplanar atom is at $a(1,0)$. The first neighbor in the layer below the one of the moving atom is at $a(0.5,0.5)$ ($a = a_0/\sqrt{2}$). The units are eV/Å^2. Vanishing force constants are not reported.

		LDA			PBE GGA		
		$-F_x$	$-F_y$	$-F_z$	$-F_x$	$-F_y$	$-F_z$
	x	−1.88		0.19	−1.42		0.11
Surface	y		0.06			0.05	
atom	z	−0.19		−0.18	−0.11		−0.08
Sub-	x	−0.54	−0.70	0.91	−0.41	−0.52	0.67
surface	y	−0.70	−0.54	0.91	−0.52	−0.41	0.67
atom	z	0.95	0.95	−1.16	0.72	0.72	−0.88
	x	−2.13			−1.60		
Bulk	y		0.12			0.08	
atom	z			0.11			0.07
Lower	x	−0.45	−0.56	0.80	−0.35	−0.41	0.60
bulk	y	−0.56	−0.45	0.80	−0.41	−0.35	0.60
atom	z	0.80	0.80	−1.00	0.60	0.60	−0.76

bor on the subsurface layer are shown. These force constants are compared with the corresponding ones in the bulk. The PBE GGA force constants between first neighbor atoms in the same layer are 11% stiffer in the bulk than on the surface. By contrast, the interactions between surface and subsurface Cu atoms are about 15–20 % stiffer than those acting in the bulk. Within LDA, the largest components of the force constant tensor are about 25% stiffer than in PBE GGA, but the 15–20 % increase of the interaction between surface and subsurface atoms with respect to the bulk is unchanged. Figure 1 shows the PBE GGA dispersions curves (continuous lines) for the phonons of a 39 layer Cu(001) slab along the $\bar{\Gamma}$-$\bar{X}$, $\bar{X}$-$\bar{M}$, and $\bar{M}$-$\bar{\Gamma}$ directions of the SBZ. The surface modes are marked with points and their frequencies are compared with the experimental data. Only surface modes whose displacements are dominant first layer are indicated. In order to identify the surface modes, **q** resolved surface phonon spectral densities (SD's) of a 107 layer slab are examined. The SD's are calculated as a sum of normalized Gaussian functions with root-mean-square deviations equal to 1.22 cm^{-1}.

Figure 2 shows the SD's calculated with PBE GGA at six points of the SBZ along the path of Fig. 1 and separated according to the polarization of the vibrational eigenmodes. SD's for modes characterized by dominant first-layer shear vertical (perpendicular to the surface) displacements and by dominant first-layer longitudinal displacements (parallel to the **q** wave vector) are plotted with continuous and dashed lines, respectively. The SD for the shear horizontal surface modes, with displacements perpendicular to the sagittal plane (defined by the surface normal and the **q** vector), is not

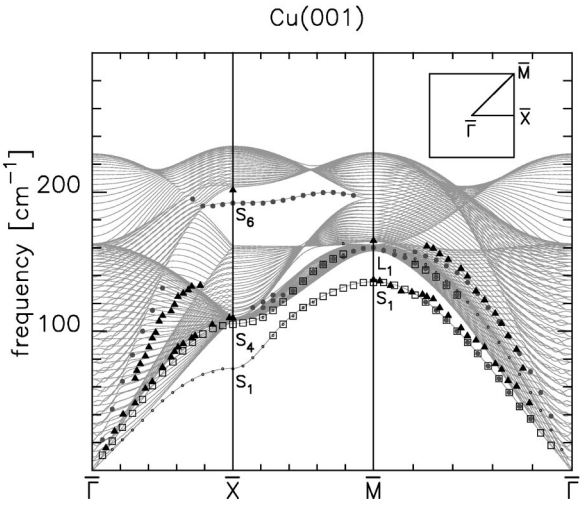

FIG. 1. Calculated PBE GGA dispersion curves for the phonons of a 39 layer Cu(001) slab compared with HAS and EELS data (solid triangles). The modes with dominant first-layer displacements are indicated. Open squares refer to shear vertical modes, open circles mark shear horizontal modes, and solid circles point to longitudinal modes (see text).

reported. All the same, these surface modes are marked with small empty circles in Fig. 1.

Along the $\bar{\Gamma}$-$\bar{X}$ direction there are three first-layer surface modes clearly identified by peaks in the SD. In this direction, modes polarizations are strictly parallel or perpendicular to the sagittal plane. The low-frequency mode S_1 is a shear horizontal mode. The mode S_4 corresponds to the Rayleigh wave (RW) with displacements predominantly perpendicular to the surface. Its frequency at $\bar{X}$ is 105 cm^{-1}. Close to the zone boundary, at 192 cm^{-1}, there is a third surface mode S_6, with longitudinal polarization. Three surface modes can be identified also along the $\bar{X}$-$\bar{M}$ direction. Here symmetry allows the mixing of S_1 and S_4 which exchange character

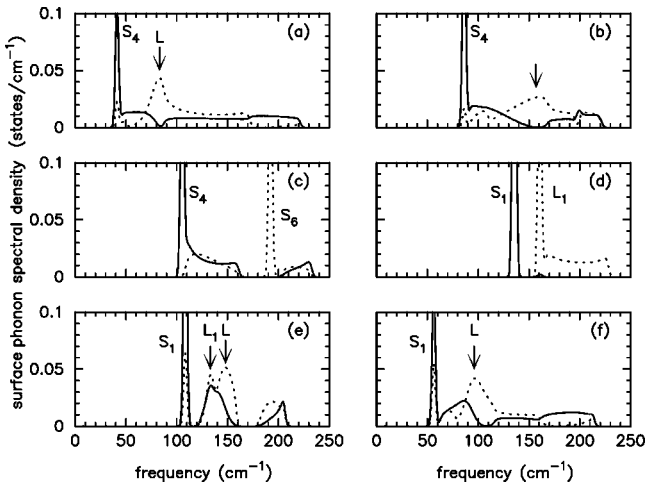

FIG. 2. The surface phonon spectral densities, at (0.143,0.0) (a), (0.321,0.0) (b), $\bar{X}$ (c), $\bar{M}$ (d), (0.316,0.316) (e), and (0.158,0.158) (f). Units are $2\pi/a_0$. Shear vertical (continuous line) and longitudinal (dashed line) polarizations are shown.

along this direction. At $\bar{M}$, the S_1 mode is the RW (with frequency 135 cm^{-1}). This mode is present also along the $\bar{M}$-$\bar{\Gamma}$ direction while the S_6 mode disappears in this direction. A new mode L_1 with longitudinal polarization appears close to $\bar{M}$. This mode enters into a region of bulk modes with the same polarization along the $\bar{M}$-$\bar{\Gamma}$ direction, and becomes weak after 2/5 of the $\bar{M}$-$\bar{\Gamma}$ path. A shear horizontal mode, not visible experimentally, with similar frequency is found along the entire $\bar{M}$-$\bar{\Gamma}$ direction. No other mode gives well defined peaks in the first-layer SD.

Experimentally, the frequencies of the RW mode along the $\bar{\Gamma}$-$\bar{X}$ and $\bar{M}$-$\bar{\Gamma}$ directions have been measured by electron energy-loss spectroscopy (EELS) and helium atom scattering (HAS).[37] In Fig. 1, I report several measured frequencies as filled triangles.[37] For the RW, the agreement between theory and experiment is good: at $\bar{X}$ and $\bar{M}$ they differ by 4 and 1 cm^{-1}. The S_6 mode measured by EELS at $\bar{X}$ is instead at 203 cm^{-1}, 11 cm^{-1} higher than the theoretical PBE GGA value. This behavior of the PBE GGA was found also in bulk Cu,[21] where the frequency of the transverse acoustic modes are in good agreement with experiment, while the frequencies of the longitudinal acoustic modes are underestimated with respect to the inelastic neutron-scattering measurements.

In addition to the modes discussed above, another peak present in the HAS cross section along the $\bar{\Gamma}$-$\bar{X}$ and $\bar{M}$-$\bar{\Gamma}$ directions has been attributed to longitudinal resonances.[37] However, the origin of these peaks is still controversial.[39] In Fig. 2, there are no well defined peaks in the SD which correspond to these modes, but the longitudinal surface phonon SD display a very broad peak. In Fig. 1, I indicate the positions of the maximum L of these peaks with small filled circles. Along $\bar{M}$-$\bar{\Gamma}$ the maximum of the longitudinal SD is found at a frequency close to the experimental points. By contrast, along $\bar{\Gamma}$-$\bar{X}$ the maximum of the SD occurs at frequencies which do not match the peak of the experimental HAS cross section. However, a more direct comparison will require the theoretical calculation of the experimental HAS cross section. As shown in Ref. 39, the shape of the interaction potential between He atoms and the Cu surface could play a role in explaining the experimental data.

Previous *ab initio* calculations,[36] limited to the $\bar{X}$ and $\bar{M}$ points of the SBZ, found a clear longitudinal resonance at the $\bar{M}$ point (L_1), and a small peak on the SD of the longitudinal modes at $\bar{X}$ at about 115 cm^{-1}. In the present calculation the presence of the L_1 mode at $\bar{M}$ is confirmed, but it is found that, along $\bar{M}$-$\bar{\Gamma}$ this mode mixes with bulk modes with the same polarizations and could possibly explain the experimental measurements only close to the $\bar{M}$ point. By contrast, the longitudinal mode at $\bar{X}$ is not present in the surface phonon SD of Fig. 2(c).

In Fig. 3, I show the dispersion curves for the phonons of a 39 layer Cu(001) slab, calculated within the LDA approximation. The modes are analyzed as the PBE GGA ones. The qualitative conclusions are the same, but quantitatively LDA overestimates all the phonon frequencies as found in the bulk.[21] The errors of the RW frequency are 11 and 18 cm^{-1} at $\bar{X}$ and $\bar{M}$, respectively. The maximum in the SD of the longitudinal modes along the $\bar{\Gamma}$-$\bar{X}$ direction is still present, but the peak is less intense than in PBE GGA, so in Fig. 3 the mode apparently disappears closer to the $\bar{\Gamma}$ point.

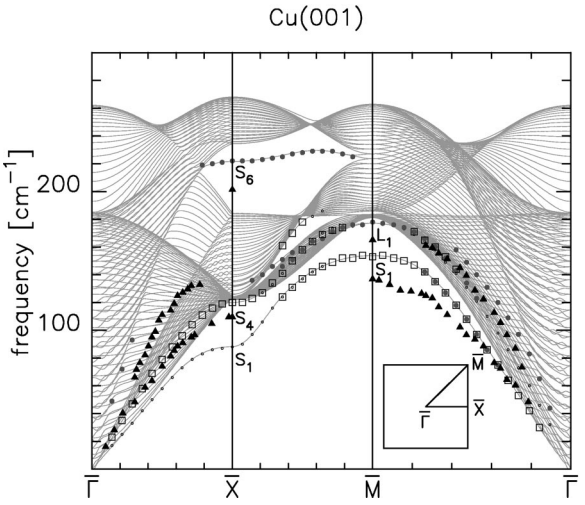

FIG. 3. Calculated LDA dispersion curves for the phonons of a 39 layer Cu(001) slab compared with HAS and EELS data (solid triangles). The modes with dominant first-layer displacements are indicated. Open squares refer to shear vertical modes, open circles mark shear horizontal modes, and solid circles point to longitudinal modes (see text).

VII. VIBRATIONAL SPECTRA OF NITROBENZENE

In this section, I address the ability of DFPT with US PP's to predict the vibrational spectra of a medium size organic molecule: nitrobenzene. In addition to the aromatic ring with five CH bonds, the molecule contains a NO_2 group. The vibrational spectra of this molecule has been measured both by infrared and by Raman spectroscopies. Vibrational frequencies calculated by quantum chemistry methods are also available (see, for instance, Refs. 41, 42, and references therein for calculations performed at the Hartree-Fock level plus correlation treated with the Møller-Plesset procedure). I simulate the molecule inside a cubic box of 22 a.u. All atoms are described by US PP's.[40] Energy cutoffs of 30 and 240 Ry have been used for the wave functions and for the charge density, respectively. The BZ is sampled by the Γ point only. The diagonal elements of the dynamical matrices are corrected to recover the acoustic sum rule. Calculations are carried out with the LDA and the PBE GGA approximations. Figure 4 shows the main parameters of the nitrobenzene geometry. The theoretical values of these parameters, obtained by relaxing the atomic positions to the minimum energy, are reported in Table II. With respect to LDA, PBE GGA expands the CO, NO, and CN bond lengths by about 0.02 Å, the CC bond lengths by 0.01 Å, and contracts the CH bonds by about 0.003 Å. The agreement with the experimental results is good in both approximations. The maximum error, which includes also the PP's error, is -0.042 Å for the CN

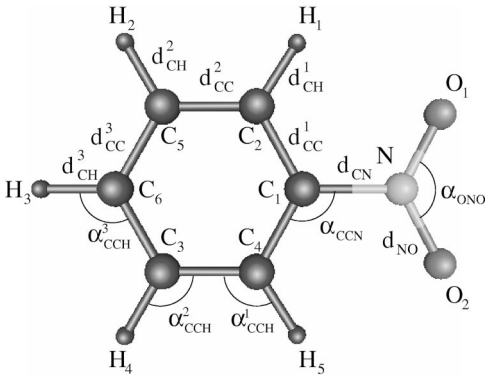

FIG. 4. Geometry of the nitrobenzene molecule. The nonequivalent bonds and angles are indicated in the figure. Their theoretical and experimental values are compared in Table II.

bond with LDA and 0.026 Å for the NO bond with PBE GGA.

Nitrobenzene has C_{2v} point group symmetry. Its 36 vibrational modes belong to the $13A_1+4A_2+12B_1+7B_2$ symmetry types. I report in Table III the frequencies calculated within LDA and PBE GGA, the mode symmetry, and a compact description of the mode eigenvectors. In some cases the displacement pattern is complex and I have not reported any indication. In other cases the assignment describes only the largest displacements. The symmetry types indicate the behavior of the displacements with respect to the symmetry operations of the C_{2v} point group: displacements of the A_1 and B_1 modes are parallel to the molecular plane, while those of the A_2 and B_2 modes are perpendicular to the molecular plane. A (B) modes are even (odd) with respect to a 180° rotation about the twofold molecular axis. In Table III, I report also the vibrational frequencies of the molecule calculated with a cutoff of 25 Ry for the wave functions and 200 Ry for the charge density. As can be seen from the table, with the present pseudopotentials,[40] this cutoff is sufficient to converge within 5 cm^{-1} the frequencies of almost all the CH bending modes but not the NO or CH stretch modes. In Table III, the frequencies deduced from infrared and Raman spectroscopies on liquid nitrobenzene are reported.[41] The frequencies of the NO_2 modes have been measured also in the gas phase[42] and since these modes are particularly sensitive to the molecular environment, in Table III, I report the gas phase values. With respect to experiment, the absolute errors of the CH stretch are larger than those of the other modes (of the order of 40 cm^{-1} for LDA and up to 72 cm^{-1} for PBE GGA). The relative error is, however, about 2%. For a few frequencies, experimentally, the mode assignment is not completely settled. For instance, different authors do not agree on the symmetry-type assignment for the out of plane CH bending modes in the 800–1000-cm^{-1} region. My assignment is in good agreement with the most recent experimental data,[41] reported in Table III. The B_1 mode experimentally reported at 1316 cm^{-1} is deduced from Ref. 41, but is not present according to Ref. 42, which suggests instead a B_1 mode at 1095 cm^{-1}, not found in my spectra. The theoretical frequencies for the mode at 1316 cm^{-1} have errors somewhat larger than the other modes (82 cm^{-1} in LDA and 43 cm^{-1} in PBE GGA). Excluding this mode as well as the CH stretch modes, the average difference between theoretical and experimental frequencies is 12 cm^{-1} both within LDA and PBE GGA. With LDA, the maximum error is 45 cm^{-1} (asymmetric stretch of NO_2), whereas with PBE-GGA it is 41 cm^{-1} (symmetric stretch of NO_2). These figures are particularly good and possibly partly fortuitous since experimental data are not corrected for anharmonicity, however, they show that DFPT with US PP's is accurate enough to be useful in interpreting the vibrational spectra of isolated organic molecules. For this particular application, the PW's basis is less efficient than other methods, but it can be competitive to study these molecules adsorbed on metallic surfaces.[43]

TABLE II. Theoretical LDA and PBE-GGA geometries of the nitrobenzene molecule. Distances are in Å and angles in degrees. The symbols are defined in Fig. 4. Experimental data are from Ref. 41. In parentheses are shown the differences on the last digit, between electron-diffraction data and microwaves (reported).

	LDA	PBE GGA	Expt.
d_{NO}	1.230	1.253	1.227 (−4)
d_{CN}	1.450	1.471	1.492 (−6)
d^1_{CC}	1.379	1.392	1.375 (21)
d^2_{CC}	1.378	1.391	1.403 (−3)
d^3_{CC}	1.383	1.395	1.396 (4)
d^1_{CH}	1.090	1.087	
d^2_{CH}	1.091	1.089	1.081 (12)
d^3_{CH}	1.092	1.089	
α_{ONO}	124.7	124.1	124.3 (10)
α_{CCN}	118.8	118.9	117.5 (8)
α^1_{CCH}	122.8	122.2	122.2
α^2_{CCH}	119.8	119.7	119.7
α^3_{CCH}	119.8	119.8	119.9

ACKNOWLEDGMENTS

I thank S. Baroni, S. de Gironcoli, F. Favot, P. Giannozzi, A. Pasquarello, E. Tosatti, and A. Baldereschi for useful discussions and collaborations. I also thank V. Bortolani for suggesting the study of the Cu(001) surface. This work has been supported by INFM (''Iniziativa trasversale calcolo parallelo'' and Sezioni F and G) and by Italian MURST (Cofin 99). Numerical calculations were performed on the Cray-T3E at CINECA in Bologna (Italy).

APPENDIX A: PERIODIC SOLIDS

In this appendix, I link the equations of the second-order energy derivatives [Eqs. (39)–(42)] with the dynamical matrices of a crystalline solid at finite **q** points of the BZ. In a crystalline solid, the atomic positions are defined by a Bravais lattice $\{\mathbf{R}_l\}$ and by the positions of the atoms, $\boldsymbol{\tau}_s$, in a reference cell. To each index I corresponds an atom identified by two indexes (l,s) with $\mathbf{R}_I=\mathbf{R}_l+\boldsymbol{\tau}_s$. In a periodic system, the wave functions are classified according to the

TABLE III. Theoretical LDA and PBE GGA frequencies of the vibrational modes of nitrobenzene. In parentheses, the errors of a calculation at 25 (200) Ry cutoffs. β denotes bending modes in the molecular plane, γ out of plane bending modes, and ν stretch modes. ν_{sy} and ν_{as} indicate the symmetric and asymmetric stretch of the NO_2 bonds. Experimental data are taken from Ref. 41. They are not corrected for anharmonic effects.

Frequency (cm^{-1})			Symmetry	Assignment
LDA	PBE GGA	Expt.		
64 (−4)	52 (0)	50	A_2	NO_2 tors.
163 (−2)	159 (0)	180	B_2	
253 (−6)	247 (−3)	265	B_1	
396 (0)	385 (−1)	399	A_1	NO_2 tr.+Ring br.
407 (−2)	404 (−1)	399	A_2	
434 (−2)	430 (0)	425	B_2	
522 (−2)	507 (−1)	532[a]	B_1	β(CN)+$\beta(NO_2)$ as.
609 (−2)	606 (0)	613	B_1	
683 (1)	669 (−1)	680	A_1	$\beta(NO_2)$ sy.+Ring br.
686 (−2)	677 (−1)	675	B_2	
703 (−2)	690 (−1)	704[a]	B_2	$\gamma(NO_2)+\gamma$(CH)
803 (−2)	788 (−1)	791	B_2	$\gamma(NO_2)+\gamma$(CH)
830 (−3)	829 (−2)	838	A_2	γ(CH)
849 (−3)	823 (−1)	853[a]	A_1	$\beta(NO_2)$
941 (−4)	937 (−2)	936	B_2	γ(CH)
976 (−4)	972 (−1)	975	A_2	γ(CH)
999 (3)	994 (−1)	990	B_2	γ(CH)
1003 (2)	994 (1)	1002	A_1	
1018 (3)	1018 (−1)	1021	A_1	β(CH)
1057 (−2)	1068 (−1)	1069	B_1	β(CH)
1102 (2)	1085 (2)	1108	A_1	ν(CN)+β(CH)
1138 (−1)	1152 (−1)	1162	B_1	β(CH)
1157 (−2)	1161 (−1)	1176	A_1	β(CH)
1274 (−2)	1292 (−1)	1308	B_1	β(CH)
1371 (−16)	1319 (−11)	1360[a]	A_1	$\nu_{sy}(NO_2)$
1401 (17)	1362 (3)	1316	B_1	ν(CC)
1449 (3)	1444 (0)	1460	B_1	
1460 (4)	1460 (0)	1480	A_1	
1593 (−25)	1538 (−18)	1548[a]	B_1	$\nu_{as}(NO_2)$
1608 (9)	1582 (2)	1588	A_1	ν(CC)
1636 (4)	1603 (0)	1612	B_1	ν(CC)
3089 (−14)	3108 (−9)	3050	A_1	ν(CH)
3098 (−13)	3119 (−7)	3080	B_1	ν(CH)
3106 (−13)	3128 (−8)	3080	A_1	ν(CH)
3119 (−12)	3152 (−9)	3080	B_1	ν(CH)
3119 (−12)	3152 (−8)	3080	A_1	ν(CH)

[a]Gas phase data.

Bloch theorem. The indexes of the energy levels i or j become double indexes $\mathbf{k},v$ where $\mathbf{k}$ is a point of the BZ, and v is a band index which denotes both filled and partially filled states. Up to now, in the text, the operators $V^{\sigma}_{KS}(\mathbf{r}_1,\mathbf{r}_2)$, $K(\mathbf{r};\mathbf{r}_1,\mathbf{r}_2)$, and $S(\mathbf{r}_1,\mathbf{r}_2)$ have been used to simplify the notation. In this appendix, I expand these operators, using their definitions in terms of the augmentation functions and the β projectors [see Eqs. (3), (5), and (8)]. As an example, I write explicitly V^{σ}_{KS} whose nonlocal part has the same form as Eq. (3) but with screened coefficients.[18] Introducing Eq. (5) in Eq. (12) and using Eq. (3) one obtains

$$V^{\sigma}_{KS}(\mathbf{r}_1,\mathbf{r}_2)=V^{\sigma}_{eff}(\mathbf{r}_1)\,\delta(\mathbf{r}_1-\mathbf{r}_2)+\sum_{Inm} D^{\sigma}_{Inm}\beta^{\gamma(I)}_{n}(\mathbf{r}_1-\mathbf{R}_I)\times\beta^{*\gamma(I)}_{m}(\mathbf{r}_2-\mathbf{R}_I), \tag{A1}$$

where the coefficients D^{σ}_{Inm} are

$$D^{\sigma}_{Inm}=D^{(0)\gamma(I)}_{nm}+\int d^3r V^{\sigma}_{eff}(\mathbf{r})Q^{\gamma(I)}_{nm}(\mathbf{r}-\mathbf{R}_I). \quad \text{(A2)}$$

The dynamical matrix, calculated at a finite $\mathbf{q}$ point of the BZ, is the Fourier transform of the interatomic force constants:

$$\Phi_{\alpha\beta}(\mathbf{q},s,s')=\frac{1}{N}\sum_{ll'} e^{-i\mathbf{q}\cdot\mathbf{R}_l}\frac{d^2F_{tot}}{d\mathbf{u}_{\alpha}(l,s)d\mathbf{u}_{\beta}(l',s')}e^{i\mathbf{q}\cdot\mathbf{R}_{l'}}, \quad \text{(A3)}$$

where $\mathbf{u}_{\alpha}(l,s)$ refers to the displacement, in the direction α, of the atom which, at equilibrium, is in $\mathbf{R}_l+\boldsymbol{\tau}_s$. N is the number of unit cells of the crystal in the Born–von Karman approach. Equations (39)–(42) yield the mixed second-order energy derivatives with respect to two perturbation parameters μ and λ. Comparing Eq. (A3) with Eqs. (39)–(42), I take μ as the displacement $\mathbf{u}_{\alpha}(l,s)$ and λ as $\mathbf{u}_{\beta}(l',s')$. To evaluate Eq. (40) one needs to solve the linear system [Eq. (29)] in order to get the change in the wave functions. The right-hand side of this system, as well as $dV^{\sigma}_{Hxc}/d\mu$ in Eq. (41), depends self-consistently on the induced charge density [Eq. (28)]. Therefore, in this Appendix, I use Eqs. (39)–(42) to write the dynamical matrices of a crystal and rewrite Eq. (28) and Eq. (29) for this purpose.

As shown, for instance, in Ref. 7, in order to calculate the dynamical matrix, it is convenient to introduce collective atomic displacements (phonons) characterized by a finite wavelength which can be commensurate or incommensurate with the underling lattice. These phonon perturbations have the following displacement pattern: in the cell identified by $\mathbf{R}_l$ the displacement of each atom is obtained from the displacement of the atoms in the reference unit cell $\mathbf{u}_{s\alpha}(\mathbf{q})$ multiplying by a $\mathbf{q}$-dependent phase factor:

$$\mathbf{u}_{\alpha}(l,s)=\mathbf{u}_{s\alpha}(\mathbf{q})e^{i\mathbf{q}\cdot\mathbf{R}_l}. \quad \text{(A4)}$$

The charge density induced by this phonon perturbation is

$$\frac{d\rho_{\sigma}(\mathbf{r})}{d\mathbf{u}_{s\alpha}(\mathbf{q})}=\sum_l e^{i\mathbf{q}\cdot\mathbf{R}_l}\frac{d\rho_{\sigma}(\mathbf{r})}{d\mathbf{u}_{\alpha}(l,s)}, \quad \text{(A5)}$$

while the change in the wave functions induced by a phonon perturbation are

$$|\Delta^{\mathbf{u}_{s\alpha}(\mathbf{q})}\psi_{\mathbf{k}v\sigma}\rangle=\sum_l e^{i\mathbf{q}\cdot\mathbf{R}_l}|\Delta^{\mathbf{u}_{\alpha}(l,s)}\psi_{\mathbf{k}v\sigma}\rangle. \quad \text{(A6)}$$

$|\Delta^{\mathbf{u}_{s\alpha}(\mathbf{q})}\psi_{\mathbf{k}v\sigma}\rangle$ is obtained from the solution of a linear system as Eq. (29), by adding, at $\mathbf{q}=0$ a term due to the Fermi energy change. By adding, with the correct phase, the linear systems for each displacement, I get the linear system for a phonon perturbation:

$$\left[-\frac{1}{2}\nabla^2+V^{\sigma}_{eff}+Q^{\sigma}+\sum_{Inm}(D^{\sigma}_{Inm}-\varepsilon_{\mathbf{k}v\sigma}q^{\gamma(I)}_{nm})|\beta^I_n\rangle\times\langle\beta^I_m|-\varepsilon_{\mathbf{k}v\sigma}\right]|\tilde{\Delta}^{\mathbf{u}_{s\alpha}(\mathbf{q})}\psi_{\mathbf{k}v\sigma}\rangle$$
$$=-P^{\dagger}_{c,\mathbf{k}v\sigma}\left[|\phi^{\mathbf{u}_{s\alpha}(\mathbf{q})}_{\mathbf{k}v\sigma}\rangle+\frac{dV^{\sigma}_{Hxc}}{d\mathbf{u}_{s\alpha}(\mathbf{q})}|\psi_{\mathbf{k}v\sigma}\rangle+\sum_{Inm}{}^3I^{\mathbf{u}_{s\alpha}(\mathbf{q})\sigma}_{Inm}|\beta^I_n\rangle\langle\beta^I_m|\psi_{\mathbf{k}v\sigma}\rangle\right], \quad \text{(A7)}$$

where the projectors $\beta^{\gamma(I)}_n(\mathbf{r}-\mathbf{R}_I)$ are written with a bra-ket notation as $|\beta^I_n\rangle$, and I defined the integral

$${}^3I^{\mathbf{u}_{s\alpha}(\mathbf{q})\sigma}_{Inm}=\int d^3r\frac{dV^{\sigma}_{Hxc}(\mathbf{r})}{d\mathbf{u}_{s\alpha}(\mathbf{q})}Q^{\gamma(I)}_{nm}(\mathbf{r}-\mathbf{R}_I). \quad \text{(A8)}$$

The change in the Hartree and exchange and correlation potential [Eq. (21)] is linear in the induced spin charge densities:

$$\frac{dV^{\sigma}_{Hxc}(\mathbf{r})}{d\mathbf{u}_{s\alpha}(\mathbf{q})}=\int d^3r_1\frac{d\rho(\mathbf{r}_1)}{d\mathbf{u}_{s\alpha}(\mathbf{q})}\frac{1}{|\mathbf{r}-\mathbf{r}_1|}+\frac{dV^{\sigma}_{xc}(\mathbf{r})}{d\mathbf{u}_{s\alpha}(\mathbf{q})}. \quad \text{(A9)}$$

In metals, the projector on the conduction band $P^{\dagger}_{c,\mathbf{k}v\sigma}$ depends on the band index, and it is the operator given in Eq. (30); in insulators $P^{\dagger}_{c,\mathbf{k}v\sigma}=P^{\dagger}_c=1-\Sigma_{\mathbf{k}'v'}|\psi_{\mathbf{k}'v'\sigma}\rangle\langle\psi_{\mathbf{k}'v'\sigma}|$.

$|\phi^{\mathbf{u}_{s\alpha}(\mathbf{q})}_{\mathbf{k}v\sigma}\rangle$ is

$$|\phi^{\mathbf{u}_{s\alpha}(\mathbf{q})}_{\mathbf{k}v\sigma}\rangle=\sum_l e^{i\mathbf{q}\cdot\mathbf{R}_l}\left(\frac{\partial V^{\sigma}_{KS}}{\partial\mathbf{u}_{\alpha}(l,s)}-\varepsilon_{\mathbf{k}v\sigma}\frac{\partial S}{\partial\mathbf{u}_{\alpha}(l,s)}\right)|\psi_{\mathbf{k}v\sigma}\rangle. \quad \text{(A10)}$$

Using Eq. (15) for the partial derivative of the KS potential and expanding the K operator, $|\phi^{\mathbf{u}_{s\alpha}(\mathbf{q})}_{\mathbf{k}v\sigma}\rangle$ is written more explicitly:

$$|\phi^{\mathbf{u}_{s\alpha}(\mathbf{q})}_{\mathbf{k}v\sigma}\rangle=\sum_l e^{i\mathbf{q}\cdot\mathbf{R}_l}\sum_{Inm}(D^{\sigma}_{Inm}-\varepsilon_{\mathbf{k}v\sigma}q^{\gamma(I)}_{nm})\left[\frac{\partial}{\partial\mathbf{u}_{\alpha}(l,s)}(|\beta^I_n\rangle\times\langle\beta^I_m|)|\psi_{\mathbf{k}v\sigma}\rangle\right]+\sum_l e^{i\mathbf{q}\cdot\mathbf{R}_l}\frac{\partial V_{loc}}{\partial\mathbf{u}_{\alpha}(l,s)}|\psi_{\mathbf{k}v\sigma}\rangle$$
$$+\sum_l e^{i\mathbf{q}\cdot\mathbf{R}_l}\sum_{Inm}\delta_{I,(l,s)}{}^1I^{\mathbf{u}_{\alpha}(l,s)\sigma}_{nm}|\beta^I_n\rangle\langle\beta^I_m|\psi_{\mathbf{k}v\sigma}\rangle+\sum_l e^{i\mathbf{q}\cdot\mathbf{R}_l}\sum_{Inm}{}^2I^{\mathbf{u}_{\alpha}(l,s)}_{Inm}|\beta^I_n\rangle\langle\beta^I_m|\psi_{\mathbf{k}v\sigma}\rangle, \quad \text{(A11)}$$

where the two integrals are

$${}^1I^{\mathbf{u}_{\alpha}(l,s)\sigma}_{nm}=\int d^3rV^{\sigma}_{eff}(\mathbf{r})\frac{\partial Q^{\gamma(I)}_{nm}(\mathbf{r}-\mathbf{R}_I)}{\partial\mathbf{u}_{\alpha}(l,s)}, \quad \text{(A12)}$$

$${}^2I^{\mathbf{u}_{\alpha}(l,s)}_{Inm}=\int d^3r\frac{\partial V_{loc}(\mathbf{r})}{\partial\mathbf{u}_{\alpha}(l,s)}Q^{\gamma(I)}_{nm}(\mathbf{r}-\mathbf{R}_I). \quad \text{(A13)}$$

Note that ^2I depends on both the atom which moves (l,s) and on the center of the augmentation function $\mathbf{R}_I$, whereas in ^1I we have $I=(l,s)$.

The induced spin charge densities are calculated via Eqs. (28) and (A5). It is useful to group together the first two terms. This is done by defining the auxiliary vector:

$$|\overline{\Delta}^{\mathbf{u}_{s\alpha}(\mathbf{q})}\psi_{\mathbf{k}v\sigma}\rangle=|\widetilde{\Delta}^{\mathbf{u}_{s\alpha}(\mathbf{q})}\psi_{\mathbf{k}v\sigma}\rangle-\frac{1}{2}\sum_{\mathbf{k}'v'}f^{\mathbf{u}_{s\alpha}(\mathbf{q})}_{\mathbf{k}v\sigma,\mathbf{k}'v'\sigma}|\psi_{\mathbf{k}'v'\sigma}\rangle+\frac{1}{2\eta}\widetilde{\delta}_{F,\mathbf{k}v\sigma}\frac{d\varepsilon_F}{d\mathbf{u}_{s\alpha}(\mathbf{q})}\delta_{\mathbf{q}0}|\psi_{\mathbf{k}v\sigma}\rangle, \quad \text{(A14)}$$

where

$$f^{\mathbf{u}_{s\alpha}(\mathbf{q})}_{\mathbf{k}v\sigma,\mathbf{k}'v'\sigma}=\sum_l e^{i\mathbf{q}\cdot\mathbf{R}_l}w_{\mathbf{k}v\sigma,\mathbf{k}'v'\sigma}\sum_{Inm}q^{\gamma(I)}_{nm}\times\langle\psi_{\mathbf{k}'v'\sigma}|\frac{\partial}{\partial\mathbf{u}_\alpha(l,s)}(|\beta^I_n\rangle\langle\beta^I_m|)|\psi_{\mathbf{k}v\sigma}\rangle, \quad \text{(A15)}$$

and the weights are

$$w_{\mathbf{k}v\sigma,\mathbf{k}'v'\sigma}=\widetilde{\theta}_{F,\mathbf{k}v\sigma}\theta_{\mathbf{k}v\sigma,\mathbf{k}'v'\sigma}+\widetilde{\theta}_{F,\mathbf{k}'v'\sigma}\theta_{\mathbf{k}'v'\sigma,\mathbf{k}v\sigma}. \quad \text{(A16)}$$

Given these definitions, the spin charge densities induced by a phonon perturbation become

$$\frac{d\rho_\sigma(\mathbf{r})}{d\mathbf{u}_{s\alpha}(\mathbf{q})}=2\sum_{\mathbf{k}v}\psi^*_{\mathbf{k}v\sigma}(\mathbf{r})\overline{\Delta}^{\mathbf{u}_{s\alpha}(\mathbf{q})}\psi_{\mathbf{k}v\sigma}(\mathbf{r})+2\sum_{\mathbf{k}v}\sum_{Inm}\times Q^{\gamma(I)}_{nm}(\mathbf{r}-\mathbf{R}_I)\langle\psi_{\mathbf{k}v\sigma}|\beta^I_n\rangle\langle\beta^I_m|\overline{\Delta}^{\mathbf{u}_{s\alpha}(\mathbf{q})}\psi_{\mathbf{k}v\sigma}\rangle+\sum_l e^{i\mathbf{q}\cdot\mathbf{R}_l}\sum_{\mathbf{k}v}\widetilde{\theta}_{F,\mathbf{k}v\sigma}\sum_{Inm}\Bigg[Q^{\gamma(I)}_{nm}(\mathbf{r}-\mathbf{R}_I)\times\langle\psi_{\mathbf{k}v\sigma}|\frac{\partial}{\partial\mathbf{u}_\alpha(l,s)}(|\beta^I_n\rangle\langle\beta^I_m|)|\psi_{\mathbf{k}v\sigma}\rangle+\frac{\partial Q^{\gamma(I)}_{nm}(\mathbf{r}-\mathbf{R}_I)}{\partial\mathbf{u}_\alpha(l,s)}\langle\psi_{\mathbf{k}v\sigma}|\beta^I_n\rangle\langle\beta^I_m|\psi_{\mathbf{k}v\sigma}\rangle\Bigg], \quad \text{(A17)}$$

where time-reversal symmetry has been used in the first two terms.

The dynamical matrix is separated into four contributions. The first term generalizes the expectation value of the mixed derivatives of the electron-ion potential [see Eq. (39)]. In the NC case, this term is diagonal in the atomic indexes s,s'. In the US PP's scheme there is a similar term:

$$\Phi^{(1a)}_{\alpha\beta}(\mathbf{q},s,s')=\frac{1}{N}\sum_l\delta_{ss'}\Bigg\{\sum_{\mathbf{k}v\sigma}\widetilde{\theta}_{F,\mathbf{k}v\sigma}\sum_{Inm}(D^\sigma_{Inm}-\varepsilon_{\mathbf{k}v\sigma}q^{\gamma(I)}_{nm})\times\langle\psi_{\mathbf{k}v\sigma}|\frac{\partial^2}{\partial\mathbf{u}_\alpha(l,s)\partial\mathbf{u}_\beta(l,s)}\times(|\beta^I_n\rangle\langle\beta^I_m|)|\psi_{\mathbf{k}v\sigma}\rangle+\int d^3r\frac{\partial^2V_{loc}(\mathbf{r})}{\partial\mathbf{u}_\alpha(l,s)\partial\mathbf{u}_\beta(l,s)}\rho(\mathbf{r})\Bigg\}, \quad \text{(A18)}$$

and another term diagonal in s and s' which contains integrals of the effective potential with the augmentation charges and their derivatives [see Eq. (38)]:

$$\Phi^{(1b)}_{\alpha\beta}(\mathbf{q},s,s')=\frac{1}{N}\sum_l\delta_{ss'}\Bigg\{\sum_{\mathbf{k}v\sigma}\widetilde{\theta}_{F,\mathbf{k}v\sigma}\sum_{Inm}\delta_{I,(l,s)}{}^4I^{\mathbf{u}_\alpha(l,s)\beta\sigma}_{nm}\times\langle\psi_{\mathbf{k}v\sigma}|\beta^I_n\rangle\langle\beta^I_m|\psi_{\mathbf{k}v\sigma}\rangle+\Bigg[\sum_{\mathbf{k}v\sigma}\widetilde{\theta}_{F,\mathbf{k}v\sigma}\sum_{Inm}{}^1I^{\mathbf{u}_\alpha(l,s)\sigma}_{nm}\langle\psi_{\mathbf{k}v\sigma}|\frac{\partial}{\partial\mathbf{u}_\beta(l,s)}\times(|\beta^I_n\rangle\langle\beta^I_m|)|\psi_{\mathbf{k}v\sigma}\rangle+(\alpha\leftrightarrow\beta)\Bigg]\Bigg\}, \quad \text{(A19)}$$

where I defined the integral

$${}^4I^{\mathbf{u}_\alpha(l,s)\beta\sigma}_{nm}=\int d^3rV^\sigma_{eff}(\mathbf{r})\frac{\partial^2Q^{\gamma(s)}_{nm}(\mathbf{r}-\mathbf{R}_I)}{\partial\mathbf{u}_\alpha(l,s)\partial\mathbf{u}_\beta(l,s)}. \quad \text{(A20)}$$

Furthermore, there is a third term [see Eq. (38)], which is nonvanishing also on the nondiagonal $s\neq s'$ elements. In fact, due to the long range of the local potential, the potential centered at one atom interacts with the augmentation charge centered at another atom:

$$\Phi^{(1c)}_{\alpha\beta}(\mathbf{q},s,s')=\frac{1}{N}\sum_{ll'}e^{-i\mathbf{q}\cdot\mathbf{R}_l}\Bigg[\sum_{\mathbf{k}v\sigma}\widetilde{\theta}_{F,\mathbf{k}v\sigma}\sum_{Inm}\delta_{I,(l's')}\times{}^5I^{\mathbf{u}_\alpha(l,s)\mathbf{u}_\beta(l',s')}_{nm}\langle\psi_{\mathbf{k}v\sigma}|\beta^I_n\rangle\langle\beta^I_m|\psi_{\mathbf{k}v\sigma}\rangle+\sum_{\mathbf{k}v\sigma}\widetilde{\theta}_{F,\mathbf{k}v\sigma}\sum_{Inm}{}^2I^{\mathbf{u}_\alpha(l,s)}_{Inm}\langle\psi_{\mathbf{k}v\sigma}|\frac{\partial}{\partial\mathbf{u}_\beta(l',s')}\times(|\beta^I_n\rangle\langle\beta^I_m|)|\psi_{\mathbf{k}v\sigma}\rangle+[\mathbf{u}_\alpha(l,s)\leftrightarrow\mathbf{u}_\beta(l',s')]\Bigg]e^{i\mathbf{q}\cdot\mathbf{R}_{l'}}, \quad \text{(A21)}$$

where

$${}^5I^{\mathbf{u}_\alpha(l,s)\mathbf{u}_\beta(l',s')}_{nm}=\int d^3r\frac{\partial V_{loc}(\mathbf{r})}{\partial\mathbf{u}_\alpha(l,s)}\frac{\partial Q^{\gamma(I)}_{nm}(\mathbf{r}-\mathbf{R}_I)}{\partial\mathbf{u}_\beta(l',s')}. \quad \text{(A22)}$$

The other parts of the dynamical matrix are easily found using the definitions introduced in this appendix. The second term is

$$\Phi^{(2)}_{\alpha\beta}(\mathbf{q},s,s')=\frac{2}{N}\sum_{\mathbf{k}v\sigma}\langle\Delta^{\mathbf{u}_{s\alpha}(\mathbf{q})}\psi_{\mathbf{k}v\sigma}|\phi^{\mathbf{u}_{s'\beta}(\mathbf{q})}_{\mathbf{k}v\sigma}\rangle. \quad \text{(A23)}$$

The third term describes the interaction of the change in V^σ_{Hxc} with the induced charge densities at fixed orbitals:

$$\Phi^{(3)}_{\alpha\beta}(\mathbf{q},s,s')=\frac{1}{N}\sum_\sigma\int d^3r\frac{dV^{*\sigma}_{Hxc}(\mathbf{r})}{d\mathbf{u}_{s\alpha}(\mathbf{q})}\Delta^{\mathbf{u}_{s'\beta}(\mathbf{q})}\rho_\sigma(\mathbf{r}), \quad \text{(A24)}$$

where $\Delta^{\mathbf{u}_{s'\beta}(\mathbf{q})}\rho_\sigma(\mathbf{r})=\Sigma_{l'}e^{i\mathbf{q}\cdot\mathbf{R}_{l'}}\Delta^{\mathbf{u}_\beta(l',s')}\rho_\sigma(\mathbf{r})$. The fourth term, due to the orthonormalization, is written as

$$\Phi^{(4)}_{\alpha\beta}(\mathbf{q},s,s') = -\frac{1}{N}\Bigg[\sum_{\mathbf{k}v\mathbf{k}'v'\sigma} f^{*\mathbf{u}_{s\alpha}(\mathbf{q})}_{\mathbf{k}v\sigma,\mathbf{k}'v'\sigma} \times \langle \psi_{\mathbf{k}'v'\sigma} | \phi^{\mathbf{u}_{s'\beta}(\mathbf{q})}_{\mathbf{k}v\sigma} \rangle + \text{H.c.}\Bigg], \quad \text{(A25)}$$

where H.c. indicates the Hermitean conjugate. In addition to these four terms, the dynamical matrix contains also two terms due to NLCC. Their expressions are given in Eq. (135) of Ref. 2.

APPENDIX B: RECIPROCAL SPACE

The equations of the previous section are not yet useful in a practical calculation because they are basis-set independent and contains sums over the unit cells indexes l and l'. In this appendix, I introduce a PW's basis set to expand the wave functions. It is well known[2] that the functions in the final expressions have the periodicity of the unperturbed lattice. The finite wavelength of the phonon is dealt with through phase factors which disappear from the final expressions. These expressions are given here.

I start with some preliminary definitions. The PW expansion of the unperturbed wave functions is

$$\psi_{\mathbf{k}v\sigma}(\mathbf{r}) = \frac{1}{\sqrt{N\Omega}} e^{i\mathbf{k}\cdot\mathbf{r}} \sum_{\mathbf{G}} c_{\mathbf{k}+\mathbf{G}v\sigma} e^{i\mathbf{G}\cdot\mathbf{r}}, \quad \text{(B1)}$$

where $\{\mathbf{G}\}$ are the reciprocal-lattice vectors of the unperturbed Bravais lattice, Ω the volume of a unit cell, and N is the number of unit cells. The first-order change in the wave functions is also expanded in PW's. For a phonon perturbation of wavelength $\mathbf{q}$, $|\Delta^{\mathbf{u}_{s\alpha}(\mathbf{q})}\psi_{\mathbf{k}v\sigma}\rangle$ is the product of a function with the periodicity of the unperturbed Bravais lattice and a phase factor $e^{i(\mathbf{k}+\mathbf{q})\cdot\mathbf{r}}$:

$$\Delta^{\mathbf{u}_{s\alpha}(\mathbf{q})}\psi_{\mathbf{k}v\sigma}(\mathbf{r}) = \frac{1}{\sqrt{N\Omega}} e^{i(\mathbf{k}+\mathbf{q})\cdot\mathbf{r}} \sum_{\mathbf{G}} d^{\mathbf{u}_{s\alpha}(\mathbf{q})}_{\mathbf{k}+\mathbf{q}+\mathbf{G}v\sigma} e^{i\mathbf{G}\cdot\mathbf{r}}. \quad \text{(B2)}$$

$\phi^{\mathbf{u}_{s\alpha}(\mathbf{q})}_{\mathbf{k}v\sigma}(\mathbf{r})$ is expanded as $\Delta^{\mathbf{u}_{s\alpha}(\mathbf{q})}\psi_{\mathbf{k}v\sigma}(\mathbf{r})$:

$$\phi^{\mathbf{u}_{s\alpha}(\mathbf{q})}_{\mathbf{k}v\sigma}(\mathbf{r}) = \frac{1}{\sqrt{N\Omega}} e^{i(\mathbf{k}+\mathbf{q})\cdot\mathbf{r}} \sum_{\mathbf{G}} p^{\mathbf{u}_{s\alpha}(\mathbf{q})}_{\mathbf{k}+\mathbf{q}+\mathbf{G}v\sigma} e^{i\mathbf{G}\cdot\mathbf{r}}. \quad \text{(B3)}$$

The US PP's are characterized by three set of functions. The β projectors [Eq. (3)], the augmentation functions [Eq. (5)], and the local potential [Eq. (6)]. None of these functions is periodic. However, using the Born–von Karman periodic boundary conditions, I assume periodicity in a very large Bravais lattice, whose unit cell contains N unit cells of the unperturbed lattice. These quantities are therefore expanded in a Fourier series. For the β functions we have

$$\beta^{\gamma(I)}_n(\mathbf{r}) = \frac{1}{N\sqrt{\Omega}} \sum_{\mathbf{k}} \sum_{\mathbf{G}} \beta^{\gamma(I)}_n(\mathbf{k}+\mathbf{G}) e^{i(\mathbf{k}+\mathbf{G})\cdot\mathbf{r}}, \quad \text{(B4)}$$

with the inverse transformation

$$\beta^{\gamma(I)}_n(\mathbf{k}+\mathbf{G}) = \frac{1}{\sqrt{\Omega}} \int d^3r \beta^{\gamma(I)}_n(\mathbf{r}) e^{-i(\mathbf{k}+\mathbf{G})\cdot\mathbf{r}}. \quad \text{(B5)}$$

Here $\mathbf{k}$ is a vector of the first BZ of the unperturbed system. A similar expansion is valid for the augmentation functions and the local potential. For instance, the augmentation functions are expanded as

$$Q^{\gamma(I)}_{nm}(\mathbf{r}) = \frac{1}{N}\sum_{\mathbf{k}} \sum_{\mathbf{G}} Q^{\gamma(I)}_{nm}(\mathbf{k}+\mathbf{G}) e^{i(\mathbf{k}+\mathbf{G})\cdot\mathbf{r}}, \quad \text{(B6)}$$

with

$$Q^{\gamma(I)}_{nm}(\mathbf{k}+\mathbf{G}) = \frac{1}{\Omega} \int d^3r Q^{\gamma(I)}_{nm}(\mathbf{r}) e^{-i(\mathbf{k}+\mathbf{G})\cdot\mathbf{r}}. \quad \text{(B7)}$$

The choice of the prefactors, in the direct and inverse Fourier transform, is a matter of definition. Their product must be $1/N\Omega$, where $N\Omega$ is the volume of the real-space integration.

In order to calculate the dynamical matrix, the induced charge density, and the linear system we need scalar products between β functions, or their derivatives and the wave functions or their first-order change. Taking $I=(l,s)$, the product $\langle \beta^I_m | \psi_{\mathbf{k}v\sigma}\rangle$can be factorized as $\langle \beta^I_m | \psi_{\mathbf{k}v\sigma}\rangle = 1/\sqrt{N}\, e^{i\mathbf{k}\cdot\mathbf{R}_l} \beta^{sm}_{\mathbf{k}v\sigma}$ where

$$\beta^{sm}_{\mathbf{k}v\sigma} = \sum_{\mathbf{G}} c_{\mathbf{k}+\mathbf{G}v\sigma} \beta^{*\gamma(s)}_m(\mathbf{k}+\mathbf{G}) e^{i(\mathbf{k}+\mathbf{G})\cdot\boldsymbol{\tau}_s} \quad \text{(B8)}$$

does not depend on the cell index l. By analogy,

$$\frac{\partial \langle \beta^I_m |}{\partial \mathbf{u}_\alpha(l,s)} | \psi_{\mathbf{k}v\sigma} \rangle = \frac{1}{\sqrt{N}} e^{i\mathbf{k}\cdot\mathbf{R}_l} \alpha^{s\alpha m}_{\mathbf{k}v\sigma}, \quad \text{(B9)}$$

with

$$\alpha^{s\alpha m}_{\mathbf{k}v\sigma} = \sum_{\mathbf{G}} c_{\mathbf{k}+\mathbf{G}v\sigma} i(\mathbf{k}+\mathbf{G})_\alpha \beta^{*\gamma(s)}_m(\mathbf{k}+\mathbf{G}) e^{i(\mathbf{k}+\mathbf{G})\cdot\boldsymbol{\tau}_s}, \quad \text{(B10)}$$

and

$$\frac{\partial^2 \langle \beta^I_m |}{\partial \mathbf{u}_\alpha(l,s)\partial \mathbf{u}_\beta(l,s)} | \psi_{\mathbf{k}v\sigma} \rangle = \frac{1}{\sqrt{N}} e^{i\mathbf{k}\cdot\mathbf{R}_l} \gamma^{s\alpha\beta m}_{\mathbf{k}v\sigma}, \quad \text{(B11)}$$

with

$$\gamma^{s\alpha\beta m}_{\mathbf{k}v\sigma} = -\sum_{\mathbf{G}} c_{\mathbf{k}+\mathbf{G}v\sigma} (\mathbf{k}+\mathbf{G})_\alpha (\mathbf{k}+\mathbf{G}) \times {}_\beta\beta^{*\gamma(s)}_m(\mathbf{k}+\mathbf{G}) e^{i(\mathbf{k}+\mathbf{G})\cdot\boldsymbol{\tau}_s}. \quad \text{(B12)}$$

The product of the β functions and the change in the wave functions has a phase factor of $\mathbf{k}+\mathbf{q}$ wavelength. With $I=(l_1,s_1)$ we have

$$\langle \beta^I_m | \overline{\Delta}^{\mathbf{u}_{s\alpha}(\mathbf{q})} \psi_{\mathbf{k}v\sigma} \rangle = \frac{1}{\sqrt{N}} e^{i(\mathbf{k}+\mathbf{q})\cdot\mathbf{R}_{l_1}} \overline{\Delta}^{\mathbf{u}_{s\alpha}(\mathbf{q})} \beta^{s_1 m}_{\mathbf{k}v\sigma}, \quad \text{(B13)}$$

where

$$\overline{\Delta}^{\mathbf{u}_{s\alpha}(\mathbf{q})}\beta^{s_1 m}_{\mathbf{k}v\sigma}=\sum_{\mathbf{G}}\ \overline{d}^{\mathbf{u}_{s\alpha}(\mathbf{q})}_{\mathbf{k}+\mathbf{q}+\mathbf{G}v\sigma}\beta^{*\gamma(s_1)}_{m}(\mathbf{k}+\mathbf{q}+\mathbf{G})e^{i(\mathbf{k}+\mathbf{q}+\mathbf{G})\cdot\boldsymbol{\tau}_{s_1}} \tag{B14}$$

does not depend on the cell index l_1. Using these scalar products, three sums over the BZ and over the filled bands are calculated. Let us define

$$a^{\mathbf{u}_{s\alpha}(\mathbf{q})\sigma}_{s_1 nm}=\frac{2}{N}\sum_{\mathbf{k}v}\ \beta^{*s_1 n}_{\mathbf{k}v\sigma}\overline{\Delta}^{\mathbf{u}_{s\alpha}(\mathbf{q})}\beta^{s_1 m}_{\mathbf{k}v\sigma}, \tag{B15}$$

$$b^{\sigma}_{snm}=\frac{1}{N}\sum_{\mathbf{k}v}\ \tilde{\theta}_{F,\mathbf{k}v\sigma}\beta^{*sn}_{\mathbf{k}v\sigma}\beta^{sm}_{\mathbf{k}v\sigma}, \tag{B16}$$

$$c^{s\alpha\sigma}_{nm}=\frac{1}{N}\sum_{\mathbf{k}v}\ \tilde{\theta}_{F,\mathbf{k}v\sigma}[\alpha^{*s\alpha n}_{\mathbf{k}v\sigma}\beta^{sm}_{\mathbf{k}v\sigma}+\beta^{*sn}_{\mathbf{k}v\sigma}\alpha^{s\alpha m}_{\mathbf{k}v\sigma}]. \tag{B17}$$

The orthonormalization terms in the induced charge density and in the dynamical matrix require the coefficients $f^{\mathbf{u}_{s\alpha}(\mathbf{q})}_{\mathbf{k}v\sigma,\mathbf{k}'v'\sigma}$ [see Eq. (A15)], which do not depend on the unit cell and are nonvanishing only if $\mathbf{k}'=\mathbf{k}+\mathbf{q}$. I therefore drop the $\mathbf{k}'$ index and write

$$f^{\mathbf{u}_{s\alpha}(\mathbf{q})}_{\mathbf{k}v\sigma v'\sigma}=w_{\mathbf{k}v\sigma v'\sigma}\sum_{nm}\ q^{\gamma(s)}_{nm}(\alpha^{*s\alpha n}_{\mathbf{k}+\mathbf{q}v'\sigma}\beta^{sm}_{\mathbf{k}v\sigma}+\beta^{*sn}_{\mathbf{k}+\mathbf{q}v'\sigma}\alpha^{s\alpha m}_{\mathbf{k}v\sigma}), \tag{B18}$$

where

$$w_{\mathbf{k}v\sigma v'\sigma}=\tilde{\theta}_{F,\mathbf{k}v\sigma}\theta_{\mathbf{k}v\sigma,\mathbf{k}+\mathbf{q}v'\sigma}+\tilde{\theta}_{F,\mathbf{k}+\mathbf{q}v'\sigma}\theta_{\mathbf{k}+\mathbf{q}v'\sigma,\mathbf{k}v\sigma}. \tag{B19}$$

The augmentation functions, or their derivatives, are integrated with the local potential or its derivatives, with the effective potential or with the variation of V^{σ}_{Hxc}. In the previous appendix, five integrals of the augmentation functions with the potentials were defined. Here, these integrals are calculated in reciprocal space and their dependence on the unit cell index is made explicit. Actually, ${}^1I^{\mathbf{u}_{\alpha}(l,s)\sigma}_{nm}$ [Eq. (A12)] does not depend on l and therefore I write it as ${}^1I^{s\alpha\sigma}_{nm}$. In reciprocal space,

$${}^1I^{s\alpha\sigma}_{nm}=\Omega\sum_{\mathbf{G}}\ i\mathbf{G}_{\alpha}V^{\sigma}_{eff}(\mathbf{G})Q^{*\gamma(s)}_{nm}(\mathbf{G})e^{i\mathbf{G}\cdot\boldsymbol{\tau}_s}. \tag{B20}$$

In order to write in reciprocal space ${}^2I^{\mathbf{u}_{\alpha}(l,s)}_{Inm}$ [Eq. (A13)], let us take $I=(l_1,s_1)$. We have ${}^2I^{\mathbf{u}_{\alpha}(l,s)}_{Inm}=(1/N)\Sigma_{\mathbf{q}}e^{-i\mathbf{q}\cdot(\mathbf{R}_l-\mathbf{R}_{l_1})}\,{}^2I^{s\alpha\mathbf{q}}_{s_1nm}$, with

$${}^2I^{s\alpha\mathbf{q}}_{s_1nm}=\Omega\sum_{\mathbf{G}}\ (-i)(\mathbf{q}+\mathbf{G})_{\alpha}Q^{*\gamma(s_1)}_{nm}(\mathbf{q}+\mathbf{G})\times e^{i(\mathbf{q}+\mathbf{G})\cdot\boldsymbol{\tau}_{s_1}}V^{\gamma(s)}_{loc}(\mathbf{q}+\mathbf{G})e^{-i(\mathbf{q}+\mathbf{G})\cdot\boldsymbol{\tau}_s}. \tag{B21}$$

Calling $I=(l_1,s_1)$, we have [Eq. (A8)] ${}^3I^{\mathbf{u}_{s\alpha}(\mathbf{q})\sigma}_{Inm}=e^{i\mathbf{q}\cdot\mathbf{R}_{l_1}}\,{}^3I^{\mathbf{u}_{s\alpha}(\mathbf{q})\sigma}_{s_1nm}$ with

$${}^3I^{\mathbf{u}_{s\alpha}(\mathbf{q})\sigma}_{s_1nm}=\Omega\sum_{\mathbf{G}}\ \frac{dV^{\sigma}_{Hxc}}{d\mathbf{u}_{s\alpha}(\mathbf{q})}(\mathbf{q}+\mathbf{G})Q^{*\gamma(s_1)}_{nm}(\mathbf{q}+\mathbf{G})e^{i(\mathbf{q}+\mathbf{G})\cdot\boldsymbol{\tau}_{s_1}}. \tag{B22}$$

${}^4I^{\mathbf{u}_{\alpha}(l,s)\beta\sigma}_{nm}$ [Eq. (A20)] does not depend on l and therefore I call it ${}^4I^{s\alpha\beta\sigma}_{nm}$ with

$${}^4I^{s\alpha\beta\sigma}_{nm}=-\Omega\sum_{\mathbf{G}}\ \mathbf{G}_{\alpha}\mathbf{G}_{\beta}V^{*\sigma}_{eff}(\mathbf{G})Q^{\gamma(s)}_{nm}(\mathbf{G})e^{-i\mathbf{G}\cdot\boldsymbol{\tau}_s}. \tag{B23}$$

In order to write in reciprocal space ${}^5I^{\mathbf{u}_{\alpha}(l,s)\mathbf{u}_{\beta}(l_1,s_1)}_{nm}$ [Eq. (A22)], it is useful to write ${}^5I^{\mathbf{u}_{\alpha}(l,s)\mathbf{u}_{\beta}(l_1,s_1)}_{nm}=(1/N)\Sigma_{\mathbf{q}}e^{i\mathbf{q}\cdot(\mathbf{R}_l-\mathbf{R}_{l_1})}\,{}^5I^{ss_1\alpha\beta\mathbf{q}}_{nm}$ where

$${}^5I^{ss_1\alpha\beta\mathbf{q}}_{nm}=\Omega\sum_{\mathbf{G}}\ (\mathbf{q}+\mathbf{G})_{\alpha}(\mathbf{q}+\mathbf{G})_{\beta}V^{*\gamma(s)}_{loc}(\mathbf{q}+\mathbf{G})\times e^{i(\mathbf{q}+\mathbf{G})\cdot\boldsymbol{\tau}_s}Q^{\gamma(s_1)}_{nm}(\mathbf{q}+\mathbf{G})e^{-i(\mathbf{q}+\mathbf{G})\cdot\boldsymbol{\tau}_{s_1}}. \tag{B24}$$

Note that only ${}^3I$ depends on the self-consistent change in V^{σ}_{Hxc}. The other integrals are calculated only once at the beginning of the self-consistent DFPT run. Note also that D^{σ}_{Inm} does not depend on l since $V_{eff}(\mathbf{r})$ is a periodic function and therefore, in the following, I shall call it D^{σ}_{snm}

Given these definitions, it is straightforward to expand the linear system [Eq. (A7)], the induced spin charge densities [Eq. (A17)], and the dynamical matrices at any $\mathbf{q}$ point [Eqs. (A18)–(A25)] in the PW basis. Consider the linear system

$$\sum_{\mathbf{G}'}\Bigg[\frac{1}{2}(\mathbf{k}+\mathbf{q}+\mathbf{G})^2\delta_{\mathbf{G}\mathbf{G}'}+V^{\sigma}_{eff}(\mathbf{G}-\mathbf{G}')+Q^{\sigma}(\mathbf{k}+\mathbf{q}+\mathbf{G},\mathbf{k}+\mathbf{q}+\mathbf{G}')-\varepsilon_{\mathbf{k}v\sigma}+\sum_{s_1nm}(D^{\sigma}_{s_1nm}-\varepsilon_{\mathbf{k}v\sigma}q^{\gamma(s_1)}_{nm})\beta^{\gamma(s_1)}_{n}(\mathbf{k}+\mathbf{q}+\mathbf{G})e^{-i\mathbf{G}\cdot\boldsymbol{\tau}_{s_1}}\times\beta^{*\gamma(s_1)}_{m}(\mathbf{k}+\mathbf{q}+\mathbf{G}')e^{i\mathbf{G}'\cdot\boldsymbol{\tau}_{s_1}}\Bigg]\tilde{d}^{\mathbf{u}_{s\alpha}(\mathbf{q})}_{\mathbf{k}+\mathbf{q}+\mathbf{G}'v\sigma}=-P^{\dagger}_{c,\mathbf{k}v\sigma}[p^{\mathbf{u}_{s\alpha}(\mathbf{q})}_{\mathbf{k}+\mathbf{q}+\mathbf{G}v\sigma}+t^{\mathbf{u}_{s\alpha}(\mathbf{q})}_{\mathbf{k}+\mathbf{q}+\mathbf{G}v\sigma}], \tag{B25}$$

where

$$Q^{\sigma}=\sum_{v'}\ \alpha_{\mathbf{k}+\mathbf{q}v'\sigma}S|\psi_{\mathbf{k}+\mathbf{q}v'\sigma}\rangle\langle\psi_{\mathbf{k}+\mathbf{q}v'\sigma}|S, \tag{B26}$$

and

$$P^{\dagger}_{c,\mathbf{k}v\sigma}=\Bigg[\tilde{\theta}_{F,\mathbf{k}v\sigma}-\sum_{v'}\ \beta_{\mathbf{k}v\sigma,\mathbf{k}+\mathbf{q}v'\sigma}S|\psi_{\mathbf{k}+\mathbf{q}v'\sigma}\rangle\langle\psi_{\mathbf{k}+\mathbf{q}v'\sigma}|\Bigg], \tag{B27}$$

with

$$\beta_{\mathbf{k}v\sigma,\mathbf{k}+\mathbf{q}v'\sigma}=\tilde{\theta}_{F,\mathbf{k}v\sigma}\theta_{\mathbf{k}v\sigma,\mathbf{k}+\mathbf{q}v'\sigma}+\tilde{\theta}_{F,\mathbf{k}+\mathbf{q}v'\sigma}\theta_{\mathbf{k}+\mathbf{q}v'\sigma,\mathbf{k}v\sigma}+\alpha_{\mathbf{k}+\mathbf{q}v'\sigma}\frac{\tilde{\theta}_{F,\mathbf{k}v\sigma}-\tilde{\theta}_{F,\mathbf{k}+\mathbf{q}v'\sigma}}{\varepsilon_{\mathbf{k}v\sigma}-\varepsilon_{\mathbf{k}+\mathbf{q}v'\sigma}}\theta_{\mathbf{k}+\mathbf{q}v'\sigma,\mathbf{k}v\sigma}. \tag{B28}$$

The right-hand side of the linear system has a non-self-consistent part [Eq. (A11)],

$$p^{\mathbf{u}_{s\alpha}(\mathbf{q})}_{\mathbf{k}+\mathbf{q}+\mathbf{G}v\sigma}=\sum_{nm}(D^{\sigma}_{snm}-\varepsilon_{\mathbf{k}v\sigma}q^{\gamma(s)}_{nm})(-i)(\mathbf{k}+\mathbf{q}+\mathbf{G})_{\alpha}\beta^{\gamma(s)}_{n}(\mathbf{k}+\mathbf{q}+\mathbf{G})e^{-i(\mathbf{k}+\mathbf{q}+\mathbf{G})\cdot\tau_s}\beta^{sm}_{\mathbf{k}v\sigma}$$
$$+\sum_{\mathbf{G}'}(-i)(\mathbf{q}+\mathbf{G}-\mathbf{G}')_{\alpha}e^{-i(\mathbf{q}+\mathbf{G}-\mathbf{G}')\cdot\tau_s}V^{\gamma(s)}_{loc}(\mathbf{q}+\mathbf{G}-\mathbf{G}')c_{\mathbf{k}+\mathbf{G}'v\sigma}+\sum_{s_1}\sum_{nm}$$
$$\times\beta^{\gamma(s_1)}_{n}(\mathbf{k}+\mathbf{q}+\mathbf{G})e^{-i(\mathbf{k}+\mathbf{q}+\mathbf{G})\cdot\tau_{s_1}}[\delta_{ss_1}((D^{\sigma}_{snm}-\varepsilon_{\mathbf{k}v\sigma}q^{\gamma(s)}_{nm})\alpha^{s\alpha m}_{\mathbf{k}v\sigma}+{}^1I^{s\alpha\sigma}_{nm}\beta^{sm}_{\mathbf{k}v\sigma})+{}^2I^{s\alpha\mathbf{q}}_{s_1nm}\beta^{s_1m}_{\mathbf{k}v\sigma}], \quad \text{(B29)}$$

and a self-consistent part

$$t^{\mathbf{u}_{s\alpha}(\mathbf{q})}_{\mathbf{k}+\mathbf{q}+\mathbf{G}v\sigma}=\sum_{\mathbf{G}'}\frac{dV^{\sigma}_{Hxc}}{d\mathbf{u}_{s\alpha}(\mathbf{q})}(\mathbf{q}+\mathbf{G}-\mathbf{G}')c_{\mathbf{k}+\mathbf{G}'v\sigma}$$
$$+\sum_{s_1}\sum_{nm}{}^3I^{\mathbf{u}_{s\alpha}(\mathbf{q})\sigma}_{s_1nm}\beta^{\gamma(s_1)}_{n}$$
$$\times(\mathbf{k}+\mathbf{q}+\mathbf{G})e^{-i(\mathbf{k}+\mathbf{q}+\mathbf{G})\cdot\tau_{s_1}}\beta^{s_1m}_{\mathbf{k}v\sigma}. \quad \text{(B30)}$$

The solution of the linear system allows the calculation of the $\mathbf{q}+\mathbf{G}$ components of the Fourier transform of the induced spin charge density [Eq. (A17)]:

$$\frac{d\rho_{\sigma}}{d\mathbf{u}_{s\alpha}(\mathbf{q})}(\mathbf{q}+\mathbf{G})=2FT_{\mathbf{q}+\mathbf{G}}\left[\sum_{\mathbf{k}v}\psi^{*}_{\mathbf{k}v\sigma}(\mathbf{r})\overline{\Delta}^{\mathbf{u}_{s\alpha}(\mathbf{q})}\psi_{\mathbf{k}v\sigma}(\mathbf{r})\right]$$
$$+\sum_{s_1}\sum_{nm}Q^{\gamma(s_1)}_{nm}(\mathbf{q}+\mathbf{G})e^{-i(\mathbf{q}+\mathbf{G})\cdot\tau_{s_1}}$$
$$\times[a^{\mathbf{u}_{s\alpha}(\mathbf{q})\sigma}_{s_1nm}+\delta_{ss_1}c^{s\alpha\sigma}_{nm}+\delta_{ss_1}(-i)$$
$$\times(\mathbf{q}+\mathbf{G})_{\alpha}b^{\sigma}_{s_1nm}], \quad \text{(B31)}$$

where the symbol $FT_{\mathbf{q}+\mathbf{G}}$ means that the first term is calculated in real space, and then the $\mathbf{q}+\mathbf{G}$ component of its Fourier transform is taken.

Finally, I discuss the dynamical matrix. Equation (A18) is similar to the one in the NC PP scheme:

$$\Phi^{(1a)}_{\alpha\beta}(\mathbf{q},s,s')=\delta_{ss'}\Bigg\{\sum_{\sigma}\sum_{mn}\frac{1}{N}\sum_{\mathbf{k}v\sigma}(D^{\sigma}_{snm}-\varepsilon_{\mathbf{k}v\sigma}q^{\gamma(s)}_{nm})$$
$$\times\tilde{\theta}_{F,\mathbf{k}v\sigma}[\gamma^{*s\alpha\beta n}_{\mathbf{k}v\sigma}\beta^{sm}_{\mathbf{k}v\sigma}+\beta^{*sn}_{\mathbf{k}v\sigma}\gamma^{s\alpha\beta m}_{\mathbf{k}v\sigma}$$
$$+\alpha^{*s\alpha n}_{\mathbf{k}v\sigma}\alpha^{s\beta m}_{\mathbf{k}v\sigma}+\alpha^{*s\beta n}_{\mathbf{k}v\sigma}\alpha^{s\alpha m}_{\mathbf{k}v\sigma}]$$
$$-\Omega\sum_{\mathbf{G}}V^{*\gamma(s)}_{loc}(\mathbf{G})e^{i\mathbf{G}\cdot\tau_s}\mathbf{G}_{\alpha}\mathbf{G}_{\beta}\rho(\mathbf{G})\Bigg\}. \quad \text{(B32)}$$

Equations (A19) and (A21) are characteristic of the US PP's scheme. The diagonal term, Eq. (A19), becomes

$$\Phi^{(1b)}_{\alpha\beta}(\mathbf{q},s,s')=\delta_{ss'}\Bigg\{\sum_{\sigma}\sum_{nm}{}^4I^{s\alpha\beta\sigma}_{nm}b^{s\sigma}_{nm}$$
$$+\left[\sum_{\sigma}\sum_{nm}{}^1I^{*s\alpha\sigma}_{nm}c^{s\beta\sigma}_{nm}+(\alpha\leftrightarrow\beta)\right]\Bigg\} \quad \text{(B33)}$$

while Eq. (A21) becomes

$$\Phi^{(1c)}_{\alpha\beta}(\mathbf{q},s,s')=\Bigg\{\Bigg[\sum_{\sigma}\sum_{nm}{}^5I^{ss'\alpha\beta\mathbf{q}}_{nm}b^{s'\sigma}_{nm}$$
$$+\sum_{\sigma}\sum_{nm}{}^2I^{*s\alpha\mathbf{q}}_{s'nm}c^{s'\beta\sigma}_{nm}\Bigg]+\text{H.c.}\Bigg\}, \quad \text{(B34)}$$

where H.c. means the Hermitean conjugate of the term in the same bracket (complex conjugate and $s\alpha$ exchanged with $s'\beta$). The second part of the dynamical matrix, similar in the NC scheme, depends on the solution of the linear system [Eq. (A23)]:

$$\Phi^{(2)}_{\alpha\beta}(\mathbf{q},s,s')=\frac{2}{N}\sum_{\mathbf{k}v\sigma}\sum_{\mathbf{G}}d^{*\mathbf{u}_{s\alpha}(\mathbf{q})}_{\mathbf{k}+\mathbf{q}+\mathbf{G}v\sigma}p^{\mathbf{u}_{s'\beta}(\mathbf{q})}_{\mathbf{k}+\mathbf{q}+\mathbf{G}v\sigma}. \quad \text{(B35)}$$

Two other terms are present only in the US PP's scheme. The interaction of the moving augmentation charge with the variation of V^{σ}_{Hxc} [Eq. (A24)] is calculated in real space integrating in a primitive cell:

$$\Phi^{(3)}_{\alpha\beta}(\mathbf{q},s,s')=\sum_{\sigma}\int_{\Omega}d^3r\frac{dV^{*\sigma}_{Hxc}(\mathbf{r})}{d\mathbf{u}_{s\alpha}(\mathbf{q})}\Delta^{\mathbf{u}_{s'\beta}(\mathbf{q})}\rho_{\sigma}(\mathbf{r}), \quad \text{(B36)}$$

where $\Delta^{\mathbf{u}_{s'\beta}(\mathbf{q})}\rho_{\sigma}(\mathbf{r})$ is calculated as in Eq. (B31) taking $\Delta^{\mathbf{u}_{s'\beta}(\mathbf{q})}\psi_{\mathbf{k}v\sigma}(\mathbf{r})=0$. Finally the term due to the change in the orthonormalization constraints [Eq. (A25)] is

$$\Phi^{(4)}_{\alpha\beta}(\mathbf{q},s,s')=-\frac{1}{N}\Bigg[\sum_{\mathbf{k}vv'\sigma}f^{*\mathbf{u}_{s\alpha}(\mathbf{q})}_{\mathbf{k}v\sigma v'\sigma}$$
$$\times\sum_{\mathbf{G}}c^{*}_{\mathbf{k}+\mathbf{q}+\mathbf{G}v'\sigma}p^{\mathbf{u}_{s'\beta}(\mathbf{q})}_{\mathbf{k}+\mathbf{q}+\mathbf{G}v\sigma}+\text{H.c.}\Bigg]. \quad \text{(B37)}$$

[1] S. Baroni, P. Giannozzi, and A. Testa, Phys. Rev. Lett. **58**, 1861 (1987).
[2] S. Baroni, S. de Gironcoli, A. Dal Corso, and P. Giannozzi, Rev. Mod. Phys. **73**, 515 (2001).
[3] X. Gonze, Phys. Rev. A **52**, 1096 (1995).
[4] P. Giannozzi and S. Baroni, J. Chem. Phys. **100**, 8537 (1994).
[5] X. Gonze, Phys. Rev. B **55**, 10 337 (1997).
[6] H. Hellmann, *Einführung in die Quantenchemie* (Deuticke, Leipzig, 1937); R. P. Feynman, Phys. Rev. **56**, 340 (1939).
[7] P. Giannozzi, S. de Gironcoli, P. Pavone, and S. Baroni, Phys. Rev. B **43**, 7231 (1991).
[8] S. de Gironcoli, Phys. Rev. B **51**, 6773 (1995).
[9] G. B. Bachelet, D. R. Hamann, and M. Schlüter, Phys. Rev. B **26**, 4199 (1982).
[10] L. Kleinman and D. M. Bylander, Phys. Rev. Lett. **48**, 1425 (1982).
[11] H. J. F. Jansen and A. J. Freeman, Phys. Rev. B **30**, 561 (1984).
[12] O. K. Andersen, Phys. Rev. B **12**, 3060 (1975).
[13] P. Blöchl, Phys. Rev. B **50**, 17 953 (1994).
[14] S. G. Louie, K. M. Ho, and M. L. Cohen, Phys. Rev. B **19**, 1774 (1979).
[15] R. Yu and H. Krakauer, Phys. Rev. B **49**, 4467 (1994).
[16] S. Y. Savrasov and D. Y. Savrasov, Phys. Rev. B **54**, 16 487 (1996).
[17] R. Heid and K.-P. Bohnen, Phys. Rev. B **60**, R7309 (1999).
[18] D. Vanderbilt, Phys. Rev. B **41**, 7892 (1990).
[19] A. Dal Corso, A. Pasquarello, and A. Baldereschi, Phys. Rev. B **56**, R11 369 (1997).
[20] S. G. Louie, S. Froyen, and M. L. Cohen, Phys. Rev. B **26**, 1738 (1982).
[21] F. Favot and A. Dal Corso, Phys. Rev. B **60**, 11 427 (1999).
[22] A. Dal Corso and S. de Gironcoli, Phys. Rev. B **62**, 273 (2000).
[23] F. Favot, A. Dal Corso, and A. Baldereschi, J. Chem. Phys. **114**, 483 (2001).
[24] P. Pulay, in *Modern Theoretical Chemistry*, edited by H. F. Schaefer (Plenum, New York, 1977); Mol. Phys. **17**, 197 (1969).
[25] The formulas presented in this paper are implemented in the PWSCF and PHONON codes, written and maintained by S. Baroni, P. Giannozzi, S. de Gironcoli, and A. Dal Corso. See www.pwscf.org.
[26] P. Hohenberg and W. Kohn, Phys. Rev. **136**, B864 (1964).
[27] J. P. Perdew and A. Zunger, Phys. Rev. B **23**, 5048 (1981).
[28] M. Weinert and J. W. Davenport, Phys. Rev. B **45**, 13 709 (1992).
[29] R. M. Wentzcovitch, J. L. Martins, and P. B. Allen, Phys. Rev. B **45**, 11 372 (1992).
[30] M. Methfessel and A. T. Paxton, Phys. Rev. B **40**, 3616 (1989).
[31] C.-L. Fu and K. M. Ho, Phys. Rev. B **28**, 5480 (1983).
[32] K. Laasonen, A. Pasquarello, R. Car, C. Lee, and D. Vanderbilt, Phys. Rev. B **47**, 10 142 (1993).
[33] X. Gonze, Phys. Rev. B **55**, 10 355 (1997).
[34] A. Dal Corso, S. Baroni, R. Resta, and S. de Gironcoli, Phys. Rev. B **47**, 3588 (1993).
[35] J. P. Perdew, K. Burke, and M. Ernzerhof, Phys. Rev. Lett. **77**, 3865 (1996).
[36] Y. Chen, S. Y. Tong, J.-S. Kim, L. L. Kesmodel, T. Rodach, K. P. Bohnen, and K. M. Ho, Phys. Rev. B **44**, 11 394 (1991).
[37] Experimental data are taken from Fig. 2 of G. Benedek, J. Ellis, N. S. Luo, A. Reichmuth, P. Ruggerone, and J. P. Toennies, Phys. Rev. B **48**, 4917 (1993).
[38] R. E. Allen, G. P. Alldredge, and F. W. de Wette, Phys. Rev. B **4**, 1648 (1971).
[39] A. Franchini, G. Santoro, V. Bortolani, A. Bellman, D. Cvetko, L. Floreano, A. Morgante, M. Peloi, F. Tommasini, and T. Zambelli, Surf. Rev. Lett. **1**, 67 (1994).
[40] Ultrasoft pseudopotentials are constructed according to the Rappe-Rabe-Kaxiras-Joannopoulos scheme with three Bessel functions as reported in G. Kresse and J. Hafner, J. Phys.: Condens. Matter **6**, 8245 (1994). The core radii, in a.u., are: C(LDA) $2s$ (1.3,1.6), $2p$ (1.3,1.6), local-$3d$ (1.3), C(PBE) $2s$ (1.2,1.6), $2p$ (1.3,1.7), local-$3d$ (1.7), O(LDA) $2s$ (1.4,1.5), $2p$ (1.4,1.6), local-$3d$ (1.4), O(PBE) $2s$ (1.4,1.7), $2p$ (1.4,1.7), local-$3d$ (1.4), N(LDA) $2s$ (1.3,1.5), $2p$ (1.4,1.6), local-$3d$ (1.1), N(PBE) $2s$ (1.3,1.5), $2p$ (1.4,1.6), local-$3d$ (1.1), H(LDA) $1s$ (1.1,1.2), local-$2p$ (1.1), H(PBE) $1s$ (1.1,1.2), local-$2p$ (1.1). Two values of the core radii indicate a channel which has been pseudized within the US-PP's scheme. In such a case, the first value is the norm-conserving core radius and the second is the US one.
[41] Experimental data are taken from Tables I and II of T. Glenewinkel-Meyer and F. F. Crim, J. Mol. Struct. **337**, 209 (1995). The reported vibrational frequencies are from the most recent source: A. Kuwae and K. Machida, Spectrochim. Acta, Part A **35**, 27 (1979).
[42] Gas phase data are taken from Table 1 of V. A. Shlyapochnikov, L. S. Khaikin, O. E. Grikina, C. W. Bock, and L. V. Vilkov, J. Mol. Struct. **326**, 1 (1994) and have been measured in G. Varsanyi, S. Holly, and L. Imre, Spectrochim. Acta, Part A **23**, 1205 (1967).
[43] F. Favot, A. Dal Corso, and A. Baldereschi, Europhys. Lett. **52**, 698 (2000).